Journal of Applied Mathematics and Mechanics

ZAMM

Zeitschrift für Angewandte Mathematik und Mechanik
Founded by Richard von Mises in 1921

Edited in cooperation with Martin-Luther-Universität Halle-Wittenberg and Gesellschaft für Angewandte Mathematik und Mechanik e. V. (GAMM)

www.zamm-journal.org

ZAMM · Z. Angew. Math. Mech. **91**, No. 2, 90 – 109 (2011) / **DOI** 10.1002/zamm.201000109

Generalized continua and non-homogeneous boundary conditions in homogenisation methods

[Plenary lecture presented at the 81st Annual GAMM Conference, Karlsruhe, 25 March 2010]

Samuel Forest* **and Duy Khanh Trinh**

MINES ParisTech, Centre des matériaux, CNRS UMR 7633, BP 87 91003 Evry Cedex, France

Received 30 May 2010, revised 10 September 2010, accepted 29 October 2010
Published online 20 December 2010

Key words Generalized continua, homogenization methods, micromorphic, second gradient.

Extensions of classical homogenization methods are presented that are used to replace a composite material by an effective generalized continuum model. Homogeneous equivalent second gradient and micromorphic models are considered, establishing links between the macroscopic generalized stress and strain measures and the fields of displacement, strain and stress inside a volume element of composite material. Recently proposed non-homogeneous boundary conditions to be applied to the unit cell, are critically reviewed. In particular, it is shown that such polynomial expansions of the local displacement field must be complemented by a generally non-periodic fluctuation field. A computational strategy is introduced to unambiguously determine this fluctuation. The approach is well-suited for elastic as well as elastoplastic composites.

1 Introduction

Generalized continua encompass higher grade media that rely on the introduction of higher order gradients of the displacement field or of some constitutive variables characterizing plasticity, damage, etc., and higher order continua that resort to additional independent kinematic or constitutive degrees of freedom. Archetypes of each type of these enhanced continuum theories are the strain gradient theory by Mindlin [42], on the one hand, and the micromorphic model by Eringen [15], on the other hand. A whole hierarchy of higher order and higher grade continua is now available to model size effects in the mechanical behaviour of materials and structures [20, 24, 31]. The micromorphic model incorporates 9 additional degrees of freedom in the three-dimensional case that represent the full rotation and distortion of a triad of directors attached to each point. It represents one of the most general formulation that can be used to address the size-dependent linear and non-linear behaviour of various materials, like solid foams as well as porous crystalline solids [13, 43].

Two major obstacles to the use of such sophisticated continuum models are the physical interpretation of the additional degrees of freedom and the identification of the numerous additional material parameters arising in the constitutive functions of the model. Generalized continua are very often referred to as media *with microstructure* without giving precisely the link between the phenomenological constitutive equations and the detailed microstructure of the material. The mechanics of heterogeneous materials and homogenization methods are widely used to derive the effective properties of classical Cauchy materials based on the description of a representative volume element. Extension of these methods to generalized continua would establish clear definitions of the macroscopic degrees of freedom and provide a systematic way of deriving additional macroscopic materials parameters. Homogenization techniques already exist to construct 1D Cosserat beam models and 2D Mindlin plate models [1]. In the case of 3D generalized continua, it has been proposed in [17, 18, 28] to construct an effective generalized continuum model starting from a heterogeneous classical Cauchy material by means of extended homogenization methods. These homogenization schemes must be clearly distinguished from another research topic which consists in considering a generalized continuum model at both the microscopic and macroscopic levels. For instance, homogenization of Cosserat composites was considered in [21, 39, 51]. The present work concentrates on the construction of an overall strain gradient or micromorphic continuum from a microscopic heterogeneous Cauchy material. Such a generalized continuum approach is necessary when significantly high strain gradients develop at the macroscopic

* Corresponding author E-mail: samuel.forest@mines-paristech.fr, Phone: +33 160 763 051, Fax: +33 160 763 150

scale, more precisely, when the wave length of variation of the macroscopic fields is not sufficiently large compared to the size of the heterogeneities.

For that purpose, quadratic boundary conditions to be applied on a RVE were first proposed in [22, 28] to construct an effective second gradient and Cosserat overall continuum, respectively. They represent extensions of the classical affine conditions used in classical homogenization theory [6]. They were used to identify higher order stiffness, typically bending stiffnesses, that are necessary to account for fiber size effect in composites under significant macroscopic strain gradients, in [2,8,9,11,44,48]. Cosserat approaches are particularly well-suited to describe the effective behaviour of civil engineering and granular materials, as shown in [5, 27, 47, 50].

Such higher order homogenisation schemes have been used in so-called FE^2 methods for which the constitutive model at each material of a computed structure is replaced by the resolution of a boundary value problem on the unit cell of the underlying heterogeneous material. The method is computationally very expensive but makes it possible to address nonlinear problems without writing explicit constitutive laws in the generalized continuum model. In [16], the Cosserat model is used at the macro-level to represent a fiber matrix composite and the quadratic and cubic boundary conditions proposed in [22] are applied to each unit cell. In the references [25, 36, 37], the macroscopic medium is regarded as a strain gradient continuum so that quadratic boundary conditions are sufficient. More recently, a micromorphic overall continuum was considered in [19, 32, 33] which represents currently the most general extension of classical homogenization models.

In most cases however, the proposed extended homogenization procedures remain heuristic and several questions are still pending: existence of a representative volume element in the presence of non-homogeneous boundary conditions, properties of the local fluctuation field in the case of a polynomial macro-field, as recently addressed by [52], and the contribution of this fluctuation in the extended Hill–Mandel condition. The objective of the present work is to illustrate that the application of polynomial loading conditions leads to a converged and well-defined energy state of the unit cell that can be used to identify effective properties of a homogeneous generalised continuum. The deviation of the local field from a polynomial distribution will be characterized in order to assess the contribution of this fluctuation to the work of internal forces of the effective medium. We do not address the validation of the approach since it has already been illustrated in the case of multilayered composites and other microstructures in [22, 33].

The article is organised as follows. Second section discusses the available homogenization techniques to construct an effective second gradient model starting from a Cauchy composite material, and points out their current shortcomings. In Sect. 3, the approach is generalized to overall micromorphic media. An extended polynomial Ansatz is proposed to prescribe the overall generalized strain measures to the unit cell. A computational strategy is described in Sect. 4 to define the notion of representative volume element in the presence of non-homogeneous boundary conditions for both elastic and elastoplastic composite materials.

Intrinsic notations are used throughout this work but the index notations is explicited at places to avoid any misunderstanding. In particular, scalars, vectors, tensors of second, third, fourth, and fifth ranks are denoted by $a, \underline{\boldsymbol{a}}, \underset{\sim}{\boldsymbol{a}}, \underline{\underline{\boldsymbol{a}}}, \underset{\approx}{\boldsymbol{a}}, \underline{\underline{\underline{\boldsymbol{a}}}}$, respectively. Contractions are written as:

$$\underset{\sim}{\boldsymbol{a}} : \underset{\sim}{\boldsymbol{b}} = a_{ij} b_{ij}, \quad \underline{\underline{\boldsymbol{a}}} \vdots \underline{\underline{\boldsymbol{b}}} = a_{ijk} b_{ijk}, \quad \underset{\approx}{\boldsymbol{a}} :: \underset{\approx}{\boldsymbol{b}} = a_{ijkl} b_{ijkl} \tag{1}$$

using the Einstein summation rule for repeated indices. The gradient operators $\boldsymbol{\nabla}_x$ or $\boldsymbol{\nabla}_X$ are introduced when the functions depend on microscopic coordinates $\underline{\boldsymbol{x}}$ or macroscopic coordinates $\underline{\boldsymbol{X}}$. The following notation is used:

$$\underline{\boldsymbol{U}} \otimes \boldsymbol{\nabla}_X = U_{i,j}\, \underline{\boldsymbol{e}}_i \otimes \underline{\boldsymbol{e}}_j, \quad \text{with} \quad U_{i,j} = \frac{\partial U_i}{\partial X_j}, \tag{2}$$

$$\underline{\boldsymbol{u}} \otimes \boldsymbol{\nabla}_x = u_{i,j}\, \underline{\boldsymbol{e}}_i \otimes \underline{\boldsymbol{e}}_j, \quad \text{with} \quad u_{i,j} = \frac{\partial u_i}{\partial x_j}, \tag{3}$$

where $(\underline{\boldsymbol{e}}_i)_{i=1,2,3}$ is a Cartesian orthonormal basis.

Throughout this work, the analysis is limited to the small deformation framework.

2 Second gradient homogenization

The objective of the homogenisation method is to replace a micro-heterogeneous Cauchy material V_∞ by a homogeneous equivalent medium with material point global coordinates $\underline{\boldsymbol{X}}$. It is assumed that a volume element $V(\underline{\boldsymbol{X}})$, of volume V, can be attached to each material point $\underline{\boldsymbol{X}}$. The points in $V(\underline{\boldsymbol{X}})$ are characterised by the local coordinates $\underline{\boldsymbol{x}}$. For simplicity, the volume elements $V(\underline{\boldsymbol{X}})$ are assumed to have the same shape. Each can be obtained by translation from a given reference unit cell $V(\underline{\boldsymbol{0}})$.

2.1 Second gradient model and asymptotic multiscale expansion method

The second gradient model relies on the introduction of the first and second gradient of the displacement field, $\underline{\boldsymbol{U}}(\underline{\boldsymbol{X}})$, in the continuum model. In particular, the work density of internal forces takes the following form

$$p^{(i)}(\underline{\boldsymbol{U}}) = \underset{\sim}{\boldsymbol{\sigma}} : \underline{\boldsymbol{U}} \otimes \boldsymbol{\nabla}_X + \underset{\approx}{\boldsymbol{M}} \vdots \underline{\boldsymbol{U}} \otimes \boldsymbol{\nabla}_X \otimes \boldsymbol{\nabla}_X, \tag{4}$$

where $\underset{\sim}{\boldsymbol{\sigma}}$ is the symmetric simple stress tensor and $\underset{\approx}{\boldsymbol{M}}$ the hyperstress or double stress tensor which is symmetric with respect to its two last indices. Note that there is a strict equivalence between the strain gradient and the second gradient of displacement models [42]. The stress tensors fulfill the following balance of momentum equation

$$\underset{\sim}{\boldsymbol{\tau}} \cdot \boldsymbol{\nabla}_X = 0, \quad \text{with} \quad \underset{\sim}{\boldsymbol{\tau}} = \underset{\sim}{\boldsymbol{\sigma}} - \underset{\approx}{\boldsymbol{M}} \cdot \boldsymbol{\nabla}_X \tag{5}$$

in the absence of volume forces nor acceleration. Constitutive relationships relate the first and second gradient of displacement to both stress tensors.

Multiscale asymptotic expansion methods have been used in [7] to derive such constitutive equations in the case of linear elastic composites with periodic microstructures. For that purpose, the local field $\underline{\boldsymbol{u}}(\underline{\boldsymbol{x}})$ inside the volume element is expanded in the form

$$\underline{\boldsymbol{u}}(\underline{\boldsymbol{x}}, \underline{\boldsymbol{X}}) = \underline{\boldsymbol{u}}_0(\underline{\boldsymbol{x}}, \underline{\boldsymbol{X}}) + \epsilon \underline{\boldsymbol{u}}_1(\underline{\boldsymbol{x}}, \underline{\boldsymbol{X}}) + \epsilon^2 \underline{\boldsymbol{u}}_2(\underline{\boldsymbol{x}}, \underline{\boldsymbol{X}}) + \epsilon^3 \underline{\boldsymbol{u}}_3(\underline{\boldsymbol{x}}, \underline{\boldsymbol{X}}) + \ldots, \tag{6}$$

where $\epsilon = l/L$ is a small parameter defined as the ratio of the typical size l of heterogeneities in the composite and the wave length L of variation of the macroscopic fields. Within this framework, the local coordinates represent a zoom $\underline{\boldsymbol{x}} = \underline{\boldsymbol{X}}/\epsilon$ around the material point $\underline{\boldsymbol{X}}$. The fields $\underline{\boldsymbol{u}}_i$ can be shown to be solutions of a sequence of boundary value problems on the unit cell yielding

$$\underline{\boldsymbol{u}}(\underline{\boldsymbol{x}}, \underline{\boldsymbol{X}}) = \underline{\boldsymbol{U}}(\underline{\boldsymbol{X}}) + \epsilon \underset{\sim}{\boldsymbol{A}}_1(\underline{\boldsymbol{x}}) : \underline{\boldsymbol{U}} \otimes \boldsymbol{\nabla}_X + \epsilon^2 \underset{\approx}{\boldsymbol{A}}_2(\underline{\boldsymbol{x}}) \vdots \underline{\boldsymbol{U}} \otimes \boldsymbol{\nabla}_X \otimes \boldsymbol{\nabla}_X + \epsilon^3 \underset{\approx}{\boldsymbol{A}}_3(\underline{\boldsymbol{x}}) :: \underline{\boldsymbol{U}} \otimes \boldsymbol{\nabla}_X \otimes \boldsymbol{\nabla}_X \otimes \boldsymbol{\nabla}_X + \ldots, \tag{7}$$

where the A_i tensors are localization tensors computed from the individual boundary value problems. They are periodic functions of the local coordinates. Applying the local constitutive law of classical linear elasticity inside the unit cell and averaging the classical Cauchy stress delivers the macroscopic higher order elastic moduli of the second gradient macroscopic medium.

In fact, the multiscale expansion method provides the effective constitutive law linking the stress $\underset{\sim}{\boldsymbol{\tau}}$ to the first, second, and third gradients of the macro-displacement field, as it should be. Indeed, if $\underset{\sim}{\boldsymbol{\sigma}}$ and $\underset{\approx}{\boldsymbol{M}}$ are linearly related to the first and second displacement gradients, it follows from the definition in (5) that $\underset{\sim}{\boldsymbol{\tau}}$ must also depend on the third displacement gradient. This fact has not been clearly recognized in the literature.

2.2 Requirements for second gradient homogenization

In the context of classical homogenization theory, for instance according to multiscale asymptotic methods, the macroscopic displacement degrees of freedom at material point $\underline{\boldsymbol{X}}$ are defined as the mean value of the local displacement field with respect to a unit cell $V(\underline{\boldsymbol{X}})$

$$\underline{\boldsymbol{U}}(\underline{\boldsymbol{X}}) = \langle \underline{\boldsymbol{u}}(\underline{\boldsymbol{x}}) \rangle_{V(\underline{\boldsymbol{X}})} = \frac{1}{V} \int_{V(\underline{\boldsymbol{X}})} \underline{\boldsymbol{u}}(\underline{\boldsymbol{x}})\, dV = \frac{1}{V} \int_{V_\infty} \underline{\boldsymbol{u}}(\underline{\boldsymbol{x}}) H_V(\underline{\boldsymbol{x}} - \underline{\boldsymbol{X}})\, dV, \tag{8}$$

where H_V is the indicator function associated with the domain $V(\underline{\boldsymbol{0}})$, taking the value 1 for points inside $V(\underline{\boldsymbol{0}})$ and 0 otherwise. As a consequence, and assuming sufficient regularity of the local displacement field, we have

$$\underline{\boldsymbol{U}} \otimes \boldsymbol{\nabla}_X = \frac{\partial \underline{\boldsymbol{U}}}{\partial \underline{\boldsymbol{X}}} = \frac{1}{V} \int_{V_\infty} \underline{\boldsymbol{u}}(\underline{\boldsymbol{x}}) \otimes \frac{\partial H_V}{\partial \underline{\boldsymbol{X}}}(\underline{\boldsymbol{x}} - \underline{\boldsymbol{X}})\, dV = \frac{1}{V} \int_{\partial V(\underline{\boldsymbol{X}})} \underline{\boldsymbol{u}}(\underline{\boldsymbol{x}}) \otimes \underline{\boldsymbol{n}}\, dV = \frac{1}{V} \int_{V(\underline{\boldsymbol{X}})} \frac{\partial \underline{\boldsymbol{u}}}{\partial \underline{\boldsymbol{x}}}\, dV, \tag{9}$$

where $\underline{\boldsymbol{n}}$ is the outer normal vector of the boundary of domain $V(\underline{\boldsymbol{X}})$, see [40] for a detailed discussion of such averaging theorems. As a result

$$\underline{\boldsymbol{U}} \otimes \boldsymbol{\nabla}_X = \langle \underline{\boldsymbol{u}} \otimes \boldsymbol{\nabla}_x \rangle_{V(\underline{\boldsymbol{X}})}. \tag{10}$$

Similarly, assuming again sufficient regularity of the local displacement field, we have

$$\underline{\boldsymbol{U}} \otimes \boldsymbol{\nabla}_X \otimes \boldsymbol{\nabla}_X = \langle \underline{\boldsymbol{u}}(\underline{\boldsymbol{x}}) \otimes \boldsymbol{\nabla}_x \otimes \boldsymbol{\nabla}_x \rangle. \tag{11}$$

A heterogeneous material can be replaced by a homogeneous second gradient model in the sense that it exists an equivalence in energy between both media in terms of the work of internal forces associated with each continuum

$$\langle \underset{\sim}{\boldsymbol{\sigma}} : \underset{\sim}{\boldsymbol{\varepsilon}} \rangle_{V(\underline{\boldsymbol{X}})} = \underset{\sim}{\boldsymbol{\Sigma}}(\underline{\boldsymbol{X}}) : \underset{\sim}{\boldsymbol{E}}(\underline{\boldsymbol{X}}) + \underset{\approx}{\boldsymbol{M}}(\underline{\boldsymbol{X}}) \vdots \underset{\approx}{\boldsymbol{K}}(\underline{\boldsymbol{X}}). \tag{12}$$

This represents an extension of the Hill–Mandel condition, well-known in classical homogenization theory [46].

The conditions (10,11,12) are the sole requirements that a generalised homogenization procedure should fulfill. In particular, prescription of generalised boundary conditions on the unit cell should not contradict the relationships (10,11) between local and overall gradient fields. Also, explicit definitions of the higher order stresses should be compatible with the condition (12).

2.3 Quadratic Ansatz

Quadratic Ansätze have been initially proposed in [14, 17, 22, 28, 38] to extend the usual affine conditions of loading of material volume element in order to incorporate strain gradient effects in the homogenization procedure. Such polynomial developments represent an alternative to multiscale asymptotic expansions to derive effective higher order properties, with the advantage that they can be used in a straightforward manner, irrespective of the local linear or nonlinear behaviour of the composite material.

Let us first consider a quadratic displacement field prescribed to the whole material volume element V

$$\underline{\boldsymbol{u}}^*(\underline{\boldsymbol{x}}) = \underset{\sim}{\boldsymbol{E}} \cdot \underline{\boldsymbol{x}} + \frac{1}{2} \underset{\approx}{\boldsymbol{D}} : (\underline{\boldsymbol{x}} \otimes \underline{\boldsymbol{x}}), \quad u_i^* = E_{ij} x_j + \frac{1}{2} D_{ijk} x_j x_k, \quad \forall \underline{\boldsymbol{x}} \in V(\underline{\boldsymbol{X}}), \tag{13}$$

where $\underset{\sim}{\boldsymbol{E}}$ is constant second order tensor and $\underset{\approx}{\boldsymbol{D}}$, having the symmetry properties $D_{ijk} = D_{ikj}$, is a constant third order tensor. When $\underline{\boldsymbol{X}}$ is taken as the geometric centre of $V(\underline{\boldsymbol{X}})$, we compute successively

$$\langle \underline{\boldsymbol{u}}^*(\underline{\boldsymbol{x}}) \otimes \boldsymbol{\nabla}_x \rangle_{V(\underline{\boldsymbol{X}})} = \underset{\sim}{\boldsymbol{E}} + \underset{\approx}{\boldsymbol{D}} \cdot \underline{\boldsymbol{X}}, \quad \langle \underline{\boldsymbol{u}}^*(\underline{\boldsymbol{x}}) \otimes \boldsymbol{\nabla}_x \otimes \boldsymbol{\nabla}_x \rangle_{V(\underline{\boldsymbol{X}})} = \underset{\approx}{\boldsymbol{D}}. \tag{14}$$

Prescribing the complete displacement field (13) can be used as an extension of the classical Voigt and Taylor homogenization models, for which the mean strain only is prescribed, in order to estimate effective second gradient properties. However, as in the classical case dealing with the homogeneous strain approximation, these estimated properties are generally too stiff. Accordingly, the quadratic conditions may be restricted to the boundary $\partial V(\underline{\boldsymbol{X}})$ of the unit cell

$$\underline{\boldsymbol{u}}(\underline{\boldsymbol{x}}) = \underline{\boldsymbol{u}}^*(\underline{\boldsymbol{x}}) = \underset{\sim}{\boldsymbol{E}} \cdot \underline{\boldsymbol{x}} + \frac{1}{2} \underset{\approx}{\boldsymbol{D}} : (\underline{\boldsymbol{x}} \otimes \underline{\boldsymbol{x}}), \quad \forall \underline{\boldsymbol{x}} \in \partial V(\underline{\boldsymbol{X}}). \tag{15}$$

This prescription entirely determines the mean strain applied to the unit cell, by virtue of the Gauss theorem

$$\begin{aligned} \langle \underline{\boldsymbol{u}}(\underline{\boldsymbol{x}}) \otimes \boldsymbol{\nabla}_x \rangle_{V(\underline{\boldsymbol{X}})} &= \frac{1}{V} \int_{\partial V(\underline{\boldsymbol{X}})} \underline{\boldsymbol{u}}(\underline{\boldsymbol{x}}) \otimes \underline{\boldsymbol{n}} \, dS = \frac{1}{V} \int_{\partial V(\underline{\boldsymbol{X}})} \underline{\boldsymbol{u}}^*(\underline{\boldsymbol{x}}) \otimes \underline{\boldsymbol{n}} \, dS \\ &= \frac{1}{V} \int_{V(\underline{\boldsymbol{X}})} \underline{\boldsymbol{u}}^*(\underline{\boldsymbol{x}}) \otimes \boldsymbol{\nabla}_x dV = \frac{1}{V} \int_{V(\underline{\boldsymbol{X}})} (\underset{\sim}{\boldsymbol{E}} + \underset{\approx}{\boldsymbol{D}} \cdot \underline{\boldsymbol{x}}) dV = \underset{\sim}{\boldsymbol{E}} + \underset{\approx}{\boldsymbol{D}} \cdot \underline{\boldsymbol{X}}. \end{aligned} \tag{16}$$

However, nothing can be said in general about the average value of the second gradient of the displacement in the material volume element

$$\langle \underline{\boldsymbol{u}}(\underline{\boldsymbol{x}}) \otimes \boldsymbol{\nabla}_x \otimes \boldsymbol{\nabla}_x \rangle_{V(\underline{\boldsymbol{X}})} = \frac{1}{V} \int_{\partial V} (\underline{\boldsymbol{u}} \otimes \boldsymbol{\nabla}_x) \otimes \underline{\boldsymbol{n}} \, dS \tag{17}$$

since the gradient of the local displacement field is not a priori known nor controlled at the boundary from the Dirichlet conditions solely. At this volume element scale, the only continuous variable is $\underline{\boldsymbol{x}}$, we do not consider the macroscopic field variable $\underline{\boldsymbol{X}}$. As a result, the use of the Dirichlet quadratic boundary conditions enables the control of the mean strain but gives only partial information on the value of its gradient $(\underline{\boldsymbol{u}} \otimes \boldsymbol{\nabla}_x)(\underline{\boldsymbol{x}})$ at the boundary. Accordingly, no information can be gained on the expected value of the average second gradient and the mean second gradient cannot be directly controlled by the coefficients of the quadratic polynomial. As a result, the condition $\langle \underline{\boldsymbol{u}} \otimes \boldsymbol{\nabla}_x \otimes \boldsymbol{\nabla}_x \rangle_V = \underset{\approx}{\boldsymbol{D}}$ must be regarded as an additional constraint to be enforced when solving the boundary value problem on the material volume element. Up to now,

to our knowledge, no numerical scheme has been proposed to enforce this additional constraint in an exact way. This will be further discussed in Sect. 2.5.

In classical homogenization, it is well-known that homogeneous strain based boundary conditions on the unit cell of a periodic medium lead to too stiff apparent moduli [34]. Periodicity boundary conditions introducing a fluctuation which is periodic at the boundary are the best-suited conditions. It is expected that such a fluctuation is also necessary in the case of quadratic loading conditions. A fluctuation field should therefore be added in the form

$$\underline{\boldsymbol{u}}(\underline{\boldsymbol{x}}) = \underset{\sim}{\boldsymbol{E}} \cdot \underline{\boldsymbol{x}} + \frac{1}{2}\underline{\underline{\boldsymbol{D}}} : (\underline{\boldsymbol{x}} \otimes \underline{\boldsymbol{x}}) + \underline{\boldsymbol{v}}(\underline{\boldsymbol{x}}), \quad u_i = E_{ij}x_j + \frac{1}{2}D_{ijk}x_jx_k + v_i, \quad \forall \underline{\boldsymbol{x}} \in V(\underline{\boldsymbol{X}}), \tag{18}$$

where $\underline{\boldsymbol{v}}(\underline{\boldsymbol{x}})$ is the fluctuation field. The fluctuation field may then contribute to the mean strain and mean strain gradient

$$\langle \underline{\boldsymbol{u}}(\underline{\boldsymbol{x}}) \otimes \boldsymbol{\nabla}_x \rangle_{V(\underline{\boldsymbol{X}})} = \underset{\sim}{\boldsymbol{E}} + \underline{\underline{\boldsymbol{D}}} \cdot \underline{\boldsymbol{X}} + \langle \underline{\boldsymbol{v}}(\underline{\boldsymbol{x}}) \otimes \boldsymbol{\nabla}_x \rangle_{V(\underline{\boldsymbol{X}})}, \tag{19}$$

$$\langle \underline{\boldsymbol{u}}(\underline{\boldsymbol{x}}) \otimes \boldsymbol{\nabla}_x \otimes \boldsymbol{\nabla}_x \rangle_{V(\underline{\boldsymbol{X}})} = \underline{\underline{\boldsymbol{D}}} + \langle \underline{\boldsymbol{v}}(\underline{\boldsymbol{x}}) \otimes \boldsymbol{\nabla}_x \otimes \boldsymbol{\nabla}_x \rangle_{V(\underline{\boldsymbol{X}})}. \tag{20}$$

If the fluctuation is periodic, meaning that it takes the same values at homologous points of the unit cell boundary, the mean first and second gradients of the fluctuation field vanish and the mean strain and strain gradient can be controlled. Such an assumption is compatible with classical first order homogenization characterized by the prescription of the $\underset{\sim}{\boldsymbol{E}}$ tensor. However there is in general no reason for assuming such a periodicity requirement in the presence of overall strain gradient loading, as discussed in [52]. On the other hand, the periodicity condition on the fluctuation field must be accompanied by corresponding static conditions in order to obtain a well-posed boundary value problem. In classical homogenization theory, the anti-periodicity of the traction vector at homologous points is required

$$\underline{\boldsymbol{v}}(\underline{\boldsymbol{x}}^-) = \underline{\boldsymbol{v}}(\underline{\boldsymbol{x}}^+), \quad \underline{\boldsymbol{t}}(\underline{\boldsymbol{x}}^+) = -\underline{\boldsymbol{t}}(\underline{\boldsymbol{x}}^-), \tag{21}$$

where $\underline{\boldsymbol{t}} = \underset{\sim}{\boldsymbol{\sigma}}^{\pm} \cdot \underline{\boldsymbol{n}}^{\pm}$ is the traction vector and $\underline{\boldsymbol{x}}^{\pm}$ are homologous points at the boundary. When a strain gradient is applied to a unit cell, the traction vectors cannot be expected to be anti-periodic any longer in general.

When the local field of displacement is expressed in the form (18), which is always possible, the extended Hill–Mandel condition (12) becomes

$$\langle \underset{\sim}{\boldsymbol{\sigma}}(\underline{\boldsymbol{x}}) : \underset{\sim}{\boldsymbol{\varepsilon}}(\underline{\boldsymbol{x}}) \rangle_{V(\underline{\boldsymbol{X}})} = \langle \underset{\sim}{\boldsymbol{\sigma}}(\underline{\boldsymbol{x}}) \rangle_{V(\underline{\boldsymbol{X}})} : \underset{\sim}{\boldsymbol{E}} + \underline{\underline{\boldsymbol{D}}} \vdots \langle \underset{\sim}{\boldsymbol{\sigma}}(\underline{\boldsymbol{x}}) \otimes \underline{\boldsymbol{x}} \rangle_{V(\underline{\boldsymbol{X}})} + \langle \underset{\sim}{\boldsymbol{\sigma}}(\underline{\boldsymbol{x}}) : \underline{\boldsymbol{v}}(\underline{\boldsymbol{x}}) \otimes \boldsymbol{\nabla}_x \rangle_{V(\underline{\boldsymbol{X}})}. \tag{22}$$

When the contribution $\langle \underset{\sim}{\boldsymbol{\sigma}}(\underline{\boldsymbol{x}}) : \underline{\boldsymbol{v}}(\underline{\boldsymbol{x}}) \otimes \boldsymbol{\nabla}_x \rangle_{V(\underline{\boldsymbol{X}})}$ of the fluctuation to the overall work of internal forces vanishes, one is entitled to propose the following definitions of the overall generalised strain and stress tensors

$$\langle \underline{\boldsymbol{u}}(\underline{\boldsymbol{x}}) \otimes \boldsymbol{\nabla}_x \rangle_{V(\underline{\boldsymbol{X}})} = \underset{\sim}{\boldsymbol{E}}, \quad \underline{\underline{\boldsymbol{K}}}(\underline{\boldsymbol{X}}) = \langle \underline{\boldsymbol{u}}(\underline{\boldsymbol{x}}) \otimes \boldsymbol{\nabla}_x \otimes \boldsymbol{\nabla}_x \rangle_{V(\underline{\boldsymbol{X}})} = \underline{\underline{\boldsymbol{D}}}, \tag{23}$$

$$\underset{\sim}{\boldsymbol{\Sigma}}(\underline{\boldsymbol{X}}) := \langle \underset{\sim}{\boldsymbol{\sigma}}(\underline{\boldsymbol{x}}) \rangle_{V(\underline{\boldsymbol{X}})}, \quad \underline{\underline{\boldsymbol{M}}}(\underline{\boldsymbol{X}}) := \langle \underset{\sim}{\boldsymbol{\sigma}}(\underline{\boldsymbol{x}}) \otimes \underline{\boldsymbol{x}} \rangle_{V(\underline{\boldsymbol{X}})} \tag{24}$$

thus relating the hyperstress tensor to the first moment of the stress distribution of the Cauchy stress field inside the material volume element. When the fluctuation field $\underline{\boldsymbol{v}}$ is periodic, its contribution to the overall work of internal forces indeed vanishes, so that the previous stress and strain definitions hold. This will be the case if $\underline{\underline{\boldsymbol{D}}} = 0$, i.e. within the classical homogenization framework. However, in general, the fluctuation is not periodic and there is also no reason for expecting the fluctuation contribution to the energy to vanish. In fact, the identifications (23) and (24) hold only if the quadratic expansion is imposed to the whole volume, as in (13). When the polynomial is prescribed at the boundary according to (18), nothing ensures that $\langle \underline{\boldsymbol{u}}(\underline{\boldsymbol{x}}) \otimes \boldsymbol{\nabla}_x \otimes \boldsymbol{\nabla}_x \rangle_{V(\underline{\boldsymbol{X}})} = \underline{\underline{\boldsymbol{D}}}$, as discussed earlier.

So, in general,

$$\langle \underset{\sim}{\boldsymbol{\sigma}}(\underline{\boldsymbol{x}}) : \underline{\boldsymbol{v}}(\underline{\boldsymbol{x}}) \otimes \boldsymbol{\nabla}_x \rangle_{V(\underline{\boldsymbol{X}})} \neq 0. \tag{25}$$

This contribution will be investigated in Sects. 4.4 and 4.5. As a result, the overall stress tensors can be defined only in an implicit way by (22).

Also, additional conditions on the fluctuations are required if the mean strain gradient is to be prescribed on the unit cell.

2.4 Links with couple stress and Cosserat approaches

The authors in [8, 9, 17, 44] adopt a restricted version of the polynomial (13) which reads, in the 2D case

$$u_1^* = -K_{31}x_1x_2 - \frac{K_{32}}{2}x_2^2, \quad u_2^* = K_{32}x_1x_2 + \frac{K_{31}}{2}x_1^2, \tag{26}$$

where the matrix K_{ij} can be interpreted as the overall curvature tensor of an effective couple stress or Cosserat medium, as proved in [22]. The couple stress theory is a special case of the second gradient model for which only the effect of the gradient of the material rotation, i.e. the skew-symmetric part of the displacement gradient, is taken into account. The Cosserat theory is obtained when the microrotation differs from the material rotation and is treated as independent degree of freedom. The Cosserat theory departs from the couple stress theory in the same way as the Timoshenko beam from the Euler-Bernoulli beam, in the 1D case. As a result, the Cosserat model possesses an additional generalized strain measure which is the difference between the microrotation and the material rotation. It has been shown in [10, 22] that this relative rotation can be prescribed to the unit cell by means of a third order polynomial that takes the following form in the 2D case

$$u_1^* = \hat{D}(x_2^3 - 3x_1^2x_2), \quad u_2^* = -\hat{D}(x_1^3 - 3x_1^2x_2), \tag{27}$$

with a single additional coefficient $\hat{D}$.

In the 3D case, it was proved in [18] that a fourth order polynomial is required to control the trace of the curvature tensor which vanishes in the 2D case and that cannot be prescribed by means of the quadratic polynomial.

2.5 Limitations of existing approaches

Analysis of available literature shows that it is difficult in general to fulfill the simultaneous conditions on the fluctuation ensuring that

$$\langle \underline{\boldsymbol{u}}\,(\underline{\boldsymbol{x}}\,) \otimes \boldsymbol{\nabla}_x \otimes \boldsymbol{\nabla}_x \rangle_{V(\underline{\boldsymbol{X}})} = \underset{\sim}{\boldsymbol{D}} \quad \text{and} \quad \langle \underset{\sim}{\boldsymbol{\sigma}}(\underline{\boldsymbol{x}}\,) : \underline{\boldsymbol{v}}\,(\underline{\boldsymbol{x}}\,) \otimes \boldsymbol{\nabla}_x \rangle_{V(\underline{\boldsymbol{X}})} = 0. \tag{28}$$

In the references [28,33,53], non homogeneous conditions are directly prescribed at the boundary of the unit cell, according to Eq. (15). As a result of the previous discussion, the mean second gradient cannot be actually controlled. In other words, there is no direct relation between the average second gradient and the coefficients of the quadratic polynomial in (15). It follows that the definition of the higher order stress (24) remains approximate.

In the special case of the bending polynomial (26) and for the specific microstructures studied in [9, 16, 22], the periodicity requirement (21) seems to be sufficient and the numerically found fluctuation field does not contribute to the overall energy. Under bending conditions, and for special symmetries of the unit cell, indeed, the anti-periodicity conditions (21) for the traction vector are still relevant. It is only approximately the case for the third order polynomial term (27) required for the full Cosserat model.

In the FE^2 strategy used in [25, 36, 37], it is essential that the requirements (28) be fulfilled. That is why these authors clearly address the question of the realization of conditions (28). They adopt the periodicity conditions (21), together with an heuristic additional linear constraint on the fluctuation $\underline{\boldsymbol{v}}$ (derived from the heuristic definition (A5) in [36]). However, this additional condition does not ensure that the mean second gradient of the displacement field is controlled by $\underset{\sim}{\boldsymbol{D}}$ in (28), as recognized by the authors. On the other hand, the condition of anti-periodic traction vector, tacitly used in these works, warrants that the fluctuation does not contribute to the overall work of internal forces, which is the second condition in (28) (condition (34) in [36]). However this anti-periodicity condition must be abandoned in the presence of overall stress and strain gradients.

The fact that usual periodic conditions (21) cannot be used in the context of second gradient homogenisation has been seen by the authors in [52] who instead propose a combination of linear and periodic perturbation terms suggested by the observation of correctors in the multiscale asymptotic expansion homogenisation method [7]. However this perturbation, though improved compared to the periodic assumption, remains approximate and confined to the use in the context of linear elasticity, for which asymptotic methods remain tractable.

Accordingly, no theoretical nor numerical scheme seems to be available in literature that is able to strictly enforce the requirements (28). Only approximate schemes have been proposed. In the present work, we will not try to enforce these conditions. Instead, using the polynomial as loading conditions in a representative volume element, we will record the evolution of the generalised contributions. This will allow for the study of the properties of the perturbation field and for the identification of effective behaviour according to an implicit scheme.

3 Micromorphic overall modelling of heterogeneous materials

The micromorphic theory first proposed by [15, 41] introduces microdeformation degrees of freedom represented by the generally non-symmetric second order tensor field, $\underset{\sim}{\boldsymbol{\chi}}(\underline{\boldsymbol{X}})$, in addition to the displacement degrees of freedom, $\underline{\boldsymbol{U}}(\underline{\boldsymbol{X}})$. It is assumed that the development of microdeformation gradient

$$\underset{\approx}{\boldsymbol{K}}(\underline{\boldsymbol{X}}) = \underset{\sim}{\boldsymbol{\chi}}(\underline{\boldsymbol{X}}) \otimes \boldsymbol{\nabla}_X \tag{29}$$

is associated with internal work and energy storage. There is also an energetic price to pay for the microdeformation to depart from the macrodeformation, characterised by the relative deformation measure

$$\underset{\sim}{\boldsymbol{e}}(\underline{\boldsymbol{X}}) = \underline{\boldsymbol{U}}(\underline{\boldsymbol{X}}) \otimes \boldsymbol{\nabla}_X - \underset{\sim}{\boldsymbol{\chi}}(\underline{\boldsymbol{X}}). \tag{30}$$

The micromorphic model encompasses the strain gradient theory as a limit case if the internal constraint

$$\underset{\sim}{\boldsymbol{\chi}} \equiv \underline{\boldsymbol{U}} \otimes \boldsymbol{\nabla}_X \quad \Longleftrightarrow \quad \underset{\sim}{\boldsymbol{e}} \equiv 0 \tag{31}$$

is enforced [20].

3.1 Definition of the micromorphic degrees of freedom

A kinematic view of the micromorphic model has been proposed by Germain [26] that we rephrase here. *In a theory which takes microstructure into account, from the macroscopic point of view of continuum mechanics, each particle is still represented by a material point* $\underline{\boldsymbol{X}}$*, but its kinematic properties are defined in a more refined way. At the microscopic level of observation, a particle appears itself as a continuum* $V(\underline{\boldsymbol{X}})$ *of small extent. Let us call* $\underline{\boldsymbol{X}}$ *its center of mass and* $\underline{\boldsymbol{x}}$ *a point of* $V(\underline{\boldsymbol{X}})$*. As* $V(\underline{\boldsymbol{X}})$ *is of small extent, it is natural to look at the Taylor expansion of the local displacement* $\underline{\boldsymbol{u}}(\underline{\boldsymbol{x}})$ *with respect to* $\underline{\boldsymbol{x}} - \underline{\boldsymbol{X}}$ *and also, as a first approximation, to stop this expansion with the terms of degree 1*

$$\underline{\boldsymbol{u}}(\underline{\boldsymbol{x}}, \underline{\boldsymbol{X}}) = \underline{\boldsymbol{U}}(\underline{\boldsymbol{X}}) + \underset{\sim}{\boldsymbol{\chi}} \cdot (\underline{\boldsymbol{x}} - \underline{\boldsymbol{X}}). \tag{32}$$

The physical significance of this assumption is clear: one postulates that one can get a sufficient description of the relative motion of the various points of the particle if one assumes that this relative motion is a homogeneous deformation. For a given local field $\underline{\boldsymbol{u}}(\underline{\boldsymbol{x}}, \underline{\boldsymbol{X}})$, in short $\underline{\boldsymbol{u}}(\underline{\boldsymbol{x}})$, instead of explicitly performing the aforementioned Taylor expansion, it has been proposed in [19, 22, 33] to determine the homogeneous deformation field (32) that is the closest to the actual displacement field, in the sense of the following minimization problem

$$\min_{\underline{\boldsymbol{U}}(\underline{\boldsymbol{X}}), \underset{\sim}{\boldsymbol{\chi}}(\underline{\boldsymbol{X}})} \int_{V(\underline{\boldsymbol{X}})} \left|\left| \underline{\boldsymbol{u}}(\underline{\boldsymbol{x}}) - \underline{\boldsymbol{U}}(\underline{\boldsymbol{X}}) - \underset{\sim}{\boldsymbol{\chi}}(\underline{\boldsymbol{X}}) \cdot (\underline{\boldsymbol{x}} - \underline{\boldsymbol{X}}) \right|\right|^2 dV \tag{33}$$

for a given material point $\underline{\boldsymbol{X}}$. The minimization procedure is straightforward and delivers, taking $\underline{\boldsymbol{X}}$ as the centre of $V(\underline{\boldsymbol{X}})$

$$\underline{\boldsymbol{U}}(\underline{\boldsymbol{X}}) = \langle \underline{\boldsymbol{u}}(\underline{\boldsymbol{x}}) \rangle_{V(\underline{\boldsymbol{X}})}, \tag{34}$$

$$\underset{\sim}{\boldsymbol{\chi}}(\underline{\boldsymbol{X}}) = \langle (\underline{\boldsymbol{u}}(\underline{\boldsymbol{x}}) - \underline{\boldsymbol{U}}(\underline{\boldsymbol{X}})) \otimes (\underline{\boldsymbol{x}} - \underline{\boldsymbol{X}}) \rangle_{V(\underline{\boldsymbol{X}})} \cdot \underset{\sim}{\boldsymbol{A}}^{-1} = \langle \underline{\boldsymbol{u}}(\underline{\boldsymbol{x}}) \otimes (\underline{\boldsymbol{x}} - \underline{\boldsymbol{X}}) \rangle_{V(\underline{\boldsymbol{X}})} \cdot \underset{\sim}{\boldsymbol{A}}^{-1} \tag{35}$$

with

$$\underset{\sim}{\boldsymbol{A}} = \langle (\underline{\boldsymbol{x}} - \underline{\boldsymbol{X}}) \otimes (\underline{\boldsymbol{x}} - \underline{\boldsymbol{X}}) \rangle_{V(\underline{\boldsymbol{X}})}. \tag{36}$$

The relation (34) is known from classical homogenization methods and defines the macroscopic displacement as the zeroth moment of the local displacement field. Formula (35) has the merit to unambiguously define the macroscopic micromorphic degrees of freedom as the first moment of the local displacement field, tensor $\underset{\sim}{\boldsymbol{A}}$ being the quadratic moment tensor of the unit cell. This represents an enhancement of the macroscopic description that incorporates additional effects of the microstructures than conventional schemes.

If the displacement field is a linear transformation, $\underline{\boldsymbol{u}} = \underset{\sim}{\boldsymbol{E}} \cdot \underline{\boldsymbol{x}}$, the microdeformation is computed as

$$\chi_{ij} = \langle u_i x_k \rangle A^{-1}_{kj} = \langle E_{il} x_l x_k \rangle A^{-1}_{kj} = E_{il} \langle x_l x_k \rangle A^{-1}_{kj} = E_{ij} \tag{37}$$

so that the microdeformation coincides with the macro-deformation $\underset{\sim}{\boldsymbol{E}}$. In particular, if a rigid body motion is applied to the unit cell, the microdeformation will reduce to the applied rotation, as it should be.

3.2 Higher order strain measures

The mechanical theory requires the evaluation of the macroscopic gradients of the degrees of freedom. The macroscopic gradient of the displacement field is still given by the average (10). The gradient of the microdeformation (29) is computed using the definition (35) as follows

$$\begin{aligned} K_{ijk} &= \frac{\partial}{\partial X_k}\left(\langle (u_i - U_i)(x_l - X_l)\rangle A^{-1}_{lj}\right) \\ &= \langle \frac{\partial}{\partial x_k}\left((u_i - U_i)(x_l - X_l)\right)\rangle A^{-1}_{lj} + \langle (u_i - U_i)(x_l - X_l)\rangle \frac{\partial}{\partial X_k} A^{-1}_{lj} \\ &= \langle u_{i,k}(x_l - X_l)\rangle A^{-1}_{lj} + \langle (u_i - U_i)\rangle A^{-1}_{kj} + \langle (u_i - U_i)(x_l - X_l)\rangle A^{-1}_{lj,k}. \end{aligned} \tag{38}$$

Taking (34) into account, and assuming that $\underset{\sim}{\boldsymbol{A}}$ does not vary from material point to material point, the microdeformation gradient takes the simple form

$$\underset{\approx}{\boldsymbol{K}}^T(\underline{\boldsymbol{X}}) = \langle \underline{\boldsymbol{u}}(\underline{\boldsymbol{x}}) \otimes \boldsymbol{\nabla}_x \otimes (\underline{\boldsymbol{x}} - \underline{\boldsymbol{X}})\rangle \cdot \underset{\sim}{\boldsymbol{A}}^{-1}, \quad K_{ijk} = \langle u_{i,k}(x_l - X_l)\rangle A^{-1}_{lj}, \tag{39}$$

where transposition of the third rank tensor is applied to the last two indices. Accordingly, the microdeformation gradient can be interpreted as the first moment of the distribution of the local displacement gradient.

The relative deformation must also be evaluated and takes the form of the difference

$$\underset{\sim}{\boldsymbol{e}}(\underline{\boldsymbol{X}}) = \langle \underline{\boldsymbol{u}}(\underline{\boldsymbol{x}}) \otimes \boldsymbol{\nabla}_x\rangle_{V(\underline{\boldsymbol{X}})} - \langle \underline{\boldsymbol{u}}(\underline{\boldsymbol{x}}) \otimes (\underline{\boldsymbol{x}} - \underline{\boldsymbol{X}})\rangle_{V(\underline{\boldsymbol{X}})} \cdot \underset{\sim}{\boldsymbol{A}}^{-1}. \tag{40}$$

When the displacement field $\underline{\boldsymbol{u}}$ is a linear transformation, inclusive rigid body motion, both the relative deformation and the microdeformation gradient vanish, as it should be.

3.3 Polynomial Ansatz

Prompted by the discussion in Sect. 2.4, we consider the following polynomial Ansatz of degree 4

$$u^*_i(\underline{\boldsymbol{x}}) = E_{ij}x_j + \frac{1}{2}D_{ijk}x_jx_k + \frac{1}{3}D_{ijkl}x_jx_kx_l + \frac{1}{4}D_{ijklm}x_jx_kx_lx_m, \quad \forall \underline{\boldsymbol{x}} \in V(0) \tag{41}$$

that is written in the following intrinsic form

$$\underline{\boldsymbol{u}}^*(\underline{\boldsymbol{x}}) = \underset{\sim}{\boldsymbol{E}} \cdot \underline{\boldsymbol{x}} + \frac{1}{2}\underset{\sim}{\boldsymbol{D}} : (\underline{\boldsymbol{x}} \otimes \underline{\boldsymbol{x}}) + \frac{1}{3}\underset{\approx}{\boldsymbol{D}} \vdots (\underline{\boldsymbol{x}} \otimes \underline{\boldsymbol{x}} \otimes \underline{\boldsymbol{x}}) + \frac{1}{4}\underset{\approx}{\underset{\sim}{\boldsymbol{D}}} :: (\underline{\boldsymbol{x}} \otimes \underline{\boldsymbol{x}} \otimes \underline{\boldsymbol{x}} \otimes \underline{\boldsymbol{x}}), \quad \forall \underline{\boldsymbol{x}} \in V(0), \tag{42}$$

where the coefficients are tensors of the ranks 2 to 5.

The macroscopic micromorphic strain measures are now computed successively for such a polynomial field on the reference unit cell $V(0)$

$$\langle \underline{\boldsymbol{u}}^* \otimes \boldsymbol{\nabla}_x\rangle_{V(0)} = \underset{\sim}{\boldsymbol{E}} + \underset{\approx}{\boldsymbol{D}} : \underset{\sim}{\boldsymbol{A}}, \tag{43}$$

$$\underset{\sim}{\boldsymbol{\chi}} = \langle \underline{\boldsymbol{u}}^* \otimes \underline{\boldsymbol{x}}\rangle_{V(0)} \cdot \underset{\sim}{\boldsymbol{A}}^{-1} = \underset{\sim}{\boldsymbol{E}} + \frac{1}{3}\underset{\approx}{\boldsymbol{D}} \vdots \underset{\approx}{\boldsymbol{A}} \cdot \underset{\sim}{\boldsymbol{A}}^{-1}, \quad \chi_{ij} = E_{ij} + \frac{1}{3}D_{ipqr}A_{pqrk}A^{-1}_{kj}, \tag{44}$$

$$\underset{\approx}{\boldsymbol{K}}^T = \underset{\approx}{\boldsymbol{D}} + \underset{\approx}{\underset{\sim}{\boldsymbol{D}}} \vdots \underset{\approx}{\boldsymbol{A}} \cdot \underset{\sim}{\boldsymbol{A}}^{-1}, \quad K_{ipq} = \langle u_{i,q}x_r\rangle_{V(0)}A^{-1}_{rp} = D_{iqp} + D_{iqklm}A_{klmr}A^{-1}_{rp}. \tag{45}$$

These simple formula hold if the coordinate system is such that $\langle \underline{\boldsymbol{x}}\rangle = \underline{\boldsymbol{X}} = \underline{\boldsymbol{0}}$, and that the means $\langle x_i\rangle$, $\langle x_ix_jx_k\rangle$, and $\langle x_ix_jx_kx_lx_m\rangle$ identically vanish. The fourth order geometric moment $\underset{\approx}{\boldsymbol{A}}$ of the unit cell has been introduced

$$\underset{\approx}{\boldsymbol{A}} = \langle \underline{\boldsymbol{x}} \otimes \underline{\boldsymbol{x}} \otimes \underline{\boldsymbol{x}} \otimes \underline{\boldsymbol{x}}\rangle_{V(0)}. \tag{46}$$

It is interesting to notice that the relative deformation is related only to the third order polynomial

$$\underset{\sim}{\boldsymbol{e}} = \underset{\approx}{\boldsymbol{D}} : \underset{\sim}{\boldsymbol{A}} - \frac{1}{3}\underset{\approx}{\boldsymbol{D}} \vdots \underset{\approx}{\boldsymbol{A}} \cdot \underset{\sim}{\boldsymbol{A}}^{-1}. \tag{47}$$

The formula (43) to (45) set direct linear relationships between the coefficients of the polynomial and the strain measures of the effective micromorphic medium. They were used in [33] to prescribe a given curvature $\underset{\sim}{\boldsymbol{K}}$ or relative deformation to the unit cell. However the number of coefficients in the polynomials generally differs from the number of components of the generalized strain measures. For instance, the microdeformation gradient K_{ipq} cannot be controlled solely by the coefficients D_{ipq} of the quadratic polynomial since D_{ipq} is symmetric with respect to the last two indices contrary to K_{ipq}. The selection of the relevant higher order polynomial coefficients remains to be done. In the present contribution, we will only consider the coefficient D_{ijk} and some coefficients of D_{ijkl}.

However, the polynomial (42) will usually not be applied to the whole volume but instead at the boundary ∂V of a given heterogeneous material volume element V

$$\underline{\boldsymbol{u}}\,(\underline{\boldsymbol{x}}\,) = \underset{\sim}{\boldsymbol{E}} \cdot \underline{\boldsymbol{x}} + \frac{1}{2}\underset{\simeq}{\boldsymbol{D}} : (\underline{\boldsymbol{x}} \otimes \underline{\boldsymbol{x}}\,) + \frac{1}{3}\underset{\approx}{\boldsymbol{D}} \vdots (\underline{\boldsymbol{x}} \otimes \underline{\boldsymbol{x}} \otimes \underline{\boldsymbol{x}}\,) + \frac{1}{4}\underset{\simeq}{\boldsymbol{D}} :: (\underline{\boldsymbol{x}} \otimes \underline{\boldsymbol{x}} \otimes \underline{\boldsymbol{x}} \otimes \underline{\boldsymbol{x}}\,), \quad \forall \underline{\boldsymbol{x}} \in \partial V. \tag{48}$$

In that case, the relation (43) is still valid but (45) must be modified. Note that the microdeformation cannot be controlled from the displacement prescribed at the boundary. The overall microdeformation gradient can be computed knowing the displacements prescribed at the boundary, using the same special coordinate system as previously, and choosing a constant translation such that $\underline{\boldsymbol{U}}\,(0) = 0$

$$\begin{aligned} K_{ipq} &= \frac{1}{V} A^{-1}_{rp} \int_{V(0)} u_{i,q} x_r \, dV = \frac{1}{V} A^{-1}_{rp} \int_{V(0)} (u_i x_r)_{,q} \, dV - \frac{1}{V} A^{-1}_{qp} \int_{V(0)} u_i \, dV \\ &= \frac{1}{V} A^{-1}_{rp} \int_{V(0)} (u_i x_r)_{,q} \, dV = \frac{1}{V} A^{-1}_{rp} \int_{\partial V(0)} u_i x_r n_q \, dS \\ &= \frac{1}{V} A^{-1}_{rp} \int_{\partial V(0)} u^*_i x_r n_q \, dS = \frac{1}{V} A^{-1}_{rp} \int_{V(0)} u^*_{i,q} x_r \, dV + \frac{1}{V} A^{-1}_{qp} \int_{V(0)} u^*_i \, dV \end{aligned} \tag{49}$$

so that the expression differs from (45) by the mean value of $\underline{\boldsymbol{u}}^*$. We find

$$\underset{\sim}{\boldsymbol{K}}^T = \underset{\approx}{\boldsymbol{D}} + \underset{\simeq}{\boldsymbol{D}} \vdots \underset{\sim}{\boldsymbol{A}} \cdot \underset{\sim}{\boldsymbol{A}}^{-1} + \tfrac{1}{2}\underset{\simeq}{\boldsymbol{D}} : \underset{\sim}{\boldsymbol{A}} \otimes \underset{\sim}{\boldsymbol{A}}^{-1} + \tfrac{1}{4}\underset{\simeq}{\boldsymbol{D}} :: \underset{\approx}{\boldsymbol{A}} \otimes \underset{\sim}{\boldsymbol{A}}^{-1}, \tag{50}$$

$$K_{ipq} = D_{iqp} + D_{iqklm} A_{klmr} A^{-1}_{rp} + \tfrac{1}{2} D_{ijk} A_{jk} A^{-1}_{qp} + \tfrac{1}{4} D_{ijklm} A_{jklm} A^{-1}_{qp}. \tag{51}$$

Finally, the real local field will be the superposition of the polynomial and of a perturbation

$$\underline{\boldsymbol{u}}\,(\underline{\boldsymbol{x}}\,) = \underline{\boldsymbol{u}}^*(\underline{\boldsymbol{x}}\,) + \underline{\boldsymbol{v}}\,(\underline{\boldsymbol{x}}\,). \tag{52}$$

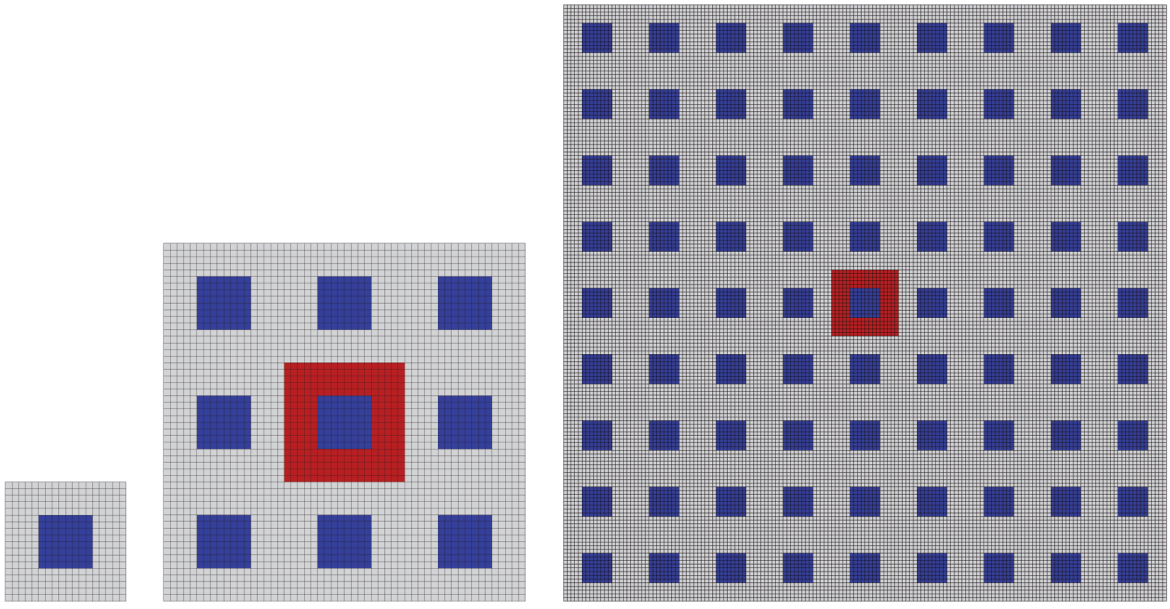

Fig. 1 (online colour at: www.zamm-journal.org) Finite Element mesh of a 1×1 unit cell (left), of a 3×3 assembly of cells (middle) and of 9×9 group of cells (right). The matrix phase is in grey and the inclusions are blue. The red colour is used to locate the central unit cell.

The fluctuation leads to additional contributions to the micromorphic measures that are obtained by substituting $\underline{\boldsymbol{v}}$ to $\underline{\boldsymbol{u}}$ in the formula (35), (39), and (40). These contributions do not vanish in general.

4 Representative volume element for polynomial Dirichlet conditions

4.1 Convergence of the energy for quadratic and cubic Ansätze in linear elastic media

The method consisting in increasing the number of unit cells in the considered volume of a periodic microstructure, subjected to polynomial boundary conditions, as illustrated in Fig. 1, has been utilized in [35] in order to show that the identified effective higher order moduli do depend on this number. We will use this numerical method in a quite different way. We consider assemblies of $N \times N$ unit cells. The number N is increased in order to apply the polynomial boundary conditions as remotely as possible from a central unit cell and reach a representative volume element size for which the energy state of the central unit does not vary any more. In that way, we are able, first, to check if such a converged state exists for several

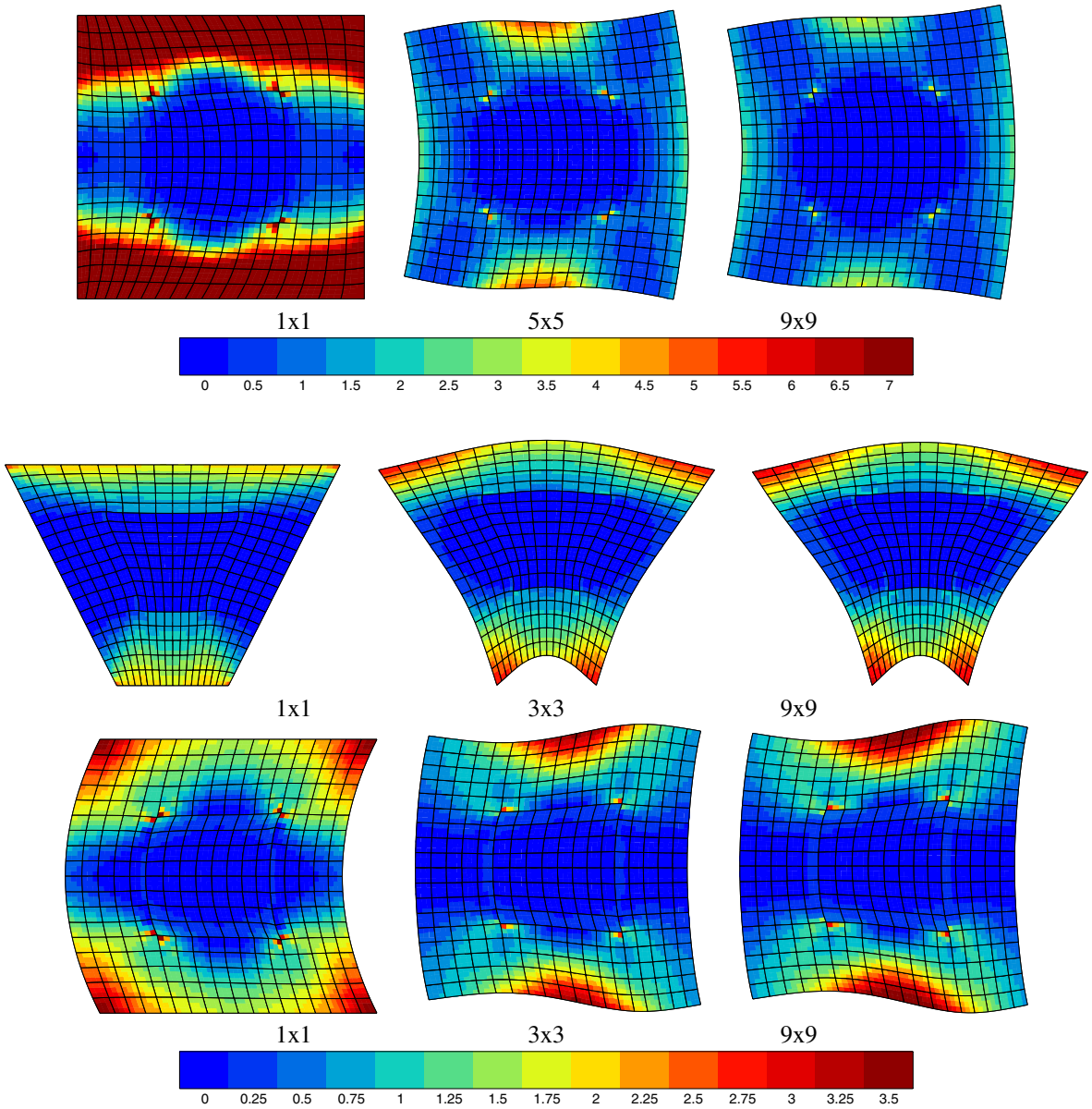

Fig. 2 (online colour at: www.zamm-journal.org) Normalised strain energy field $W(\underline{\boldsymbol{x}})/\overline{W}$ in the central unit cell when applying quadratic Dirichlet boundary conditions (15) at the remote boundary of a $N \times N$ group of cells, for $D_{111} = 1$ mm^{-1} (top), $D_{112} = 1$ mm^{-1} (middle), $D_{122} = 1$ mm^{-1} (bottom). The considered material is the composite of Fig. 1.

kinds of polynomials, and, second, to fully characterize the deviation of the actual displacement field from the applied polynomial field.

As an example, a periodic composite is considered with the unit cell of Fig. 1 (left) consisting of a square cell with a square inclusion at the center. Assemblies of 3×3 and 9×9 cells are also illustrated in Fig. 1. Both materials are assumed to behave elastically, the grid material being the hard phase (Young's modulus $E = 200000$ MPa), whereas the inclusions are soft ($E = 20000$ MPa). The Poisson ratio is identical for both materials: $\nu = 0.3$. The volume fraction of inclusions is 20%. The edge length of the unit cell is 1 mm. Larger assemblies are multiples of this length. Plane strain conditions are enforced in the following finite element computations. Eight-node quadratic square elements, with nine Gauss points, are used throughout this work.

The outer boundary of assemblies of $1 \times 1,\ 3 \times 3,\ 5 \times 5, \ldots, 9 \times 9$ cells has been subjected to the quadratic Dirichlet boundary conditions from (15) by successively setting $D_{111} = 1\ \mathrm{mm}^{-1}$, $D_{112} = 1\ \mathrm{mm}^{-1}$, $D_{122} = 1\ \mathrm{mm}^{-1}$, the remaining coefficient being set to zero. These coefficients are the relevant ones for the 2D case. In Fig. 2, we show the field of normalized elastic work $W(\underline{\boldsymbol{x}})/\overline{W}$, where $W(\underline{\boldsymbol{x}}) = \underset{\sim}{\boldsymbol{\sigma}}(\underline{\boldsymbol{x}}) : \underset{\sim}{\boldsymbol{\varepsilon}}(\underline{\boldsymbol{x}})$ is the local work of internal forces and $\overline{W} = \langle \underset{\sim}{\boldsymbol{\sigma}} : \underset{\sim}{\boldsymbol{\varepsilon}} \rangle_{9\times 9}$ is the average elastic work in the central cell of the 9×9 assembly, as a consequence of the non-homogeneous Dirichlet conditions. It turns ouht that, for the three loading conditions, there exists a converged field of elastic energy in the central cell. This stable state is obtained for the 5×5 or larger assemblies. The quadratic conditions induce strong boundary layer effects that do not disturb the field in the central cell if the outer boundary is remote enough. This property is akin to the classical notion of representative volume element.

As shown by the deformed states of Fig. 2(left), the edges of the outer boundary remain straight or become parabolic. In contrast, the edges of the central cells are no longer straight lines nor parabolic but exhibit an additional waviness corresponding to a perturbation $\underline{\boldsymbol{v}}\,(\underline{\boldsymbol{x}}\,)$ of the polynomial field. Note in particular the type of bending deformation induced by the loading D_{112}.

We have also checked that there exists a converged state when the cubic polynomial (27) is prescribed at the outer boundary as shown in Fig. 3.

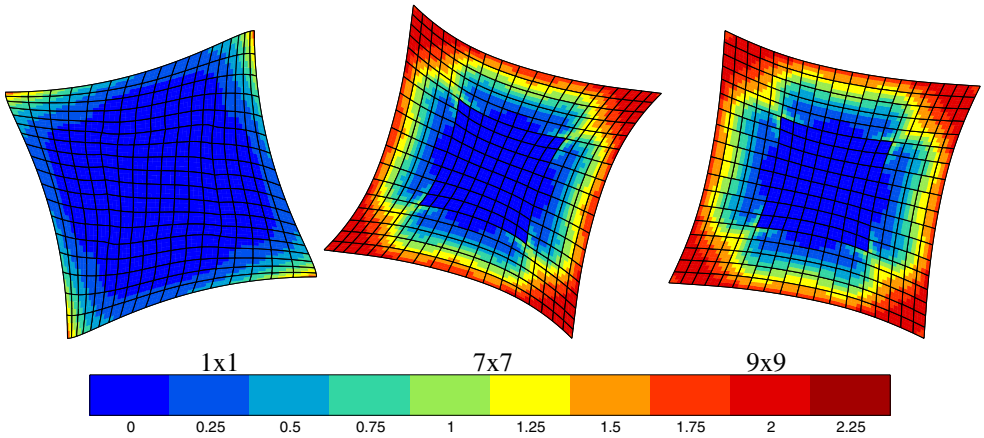

Fig. 3 (online colour at: www.zamm-journal.org) Normalised strain energy field $W(\underline{\boldsymbol{x}})/\overline{W}$ in the central unit cell when applying the cubic Dirichlet boundary conditions (27) at the remote boundary of a $N \times N$ group of cells, for $\hat{D} = 1$. The considered material is the composite of Fig. 1.

Table 1 Overall microdeformation gradient components induced on the central unit cell by the successive application of quadratic polynomial coefficient at the remote boundary of a cell assembly.

	$D_{111} = 1\ \mathrm{mm}^{-1}$	$D_{112} = 1\ \mathrm{mm}^{-1}$	$D_{122} = 1\ \mathrm{mm}^{-1}$
K_{111}	0.037	0.	−0.276
K_{112}	0.	1.070	0.
K_{122}	−0.434	0.	0.474
K_{211}	0.	−0.820	0.
K_{212}	0.122	0.	0.172
K_{222}	0.	−0.688	0.

We find that the mean strain in the central unit cell is zero for the considered quadratic and cubic boundary conditions, as it should be. The microdeformation gradient components K_{ijk} induced by the application of the polynomial D_{ijk} can be computed as a post-processing using the definition (39) applied to the converged state of the central unit cell. The corresponding values are given in Table 1. It appears that one single non-vanishing term of the polynomial leads to several non-zero components of the microdeformation gradient. For instance, the coefficient D_{112} induces a main K_{112} contribution but also comparable K_{211} and K_{222} contributions. The loading D_{111} induces mainly K_{122} and K_{212} components. Due to the linearity of the problem with respect to the coefficients of the polynomial, it is possible to determine a combination of D_{ijk} values that leads to the wanted microdeformation gradient components and thus it is possible to control $\underset{\sim}{\boldsymbol{K}}$ on the unit cell.

4.2 Particular case of a micro-homogeneous medium

The linear polynomial $u_i^* = E_{ij}x_j$ of classical homogenisation displays the remarkable property that, when applied to the boundary of a volume element made of a homogeneous material, the solution of the boundary value problem is the linear polynomial u_i^* itself. In other words, the fluctuation $\underline{\boldsymbol{v}}$ in (18) vanishes if the medium is homogeneous. Does this property pertain to higher orders?

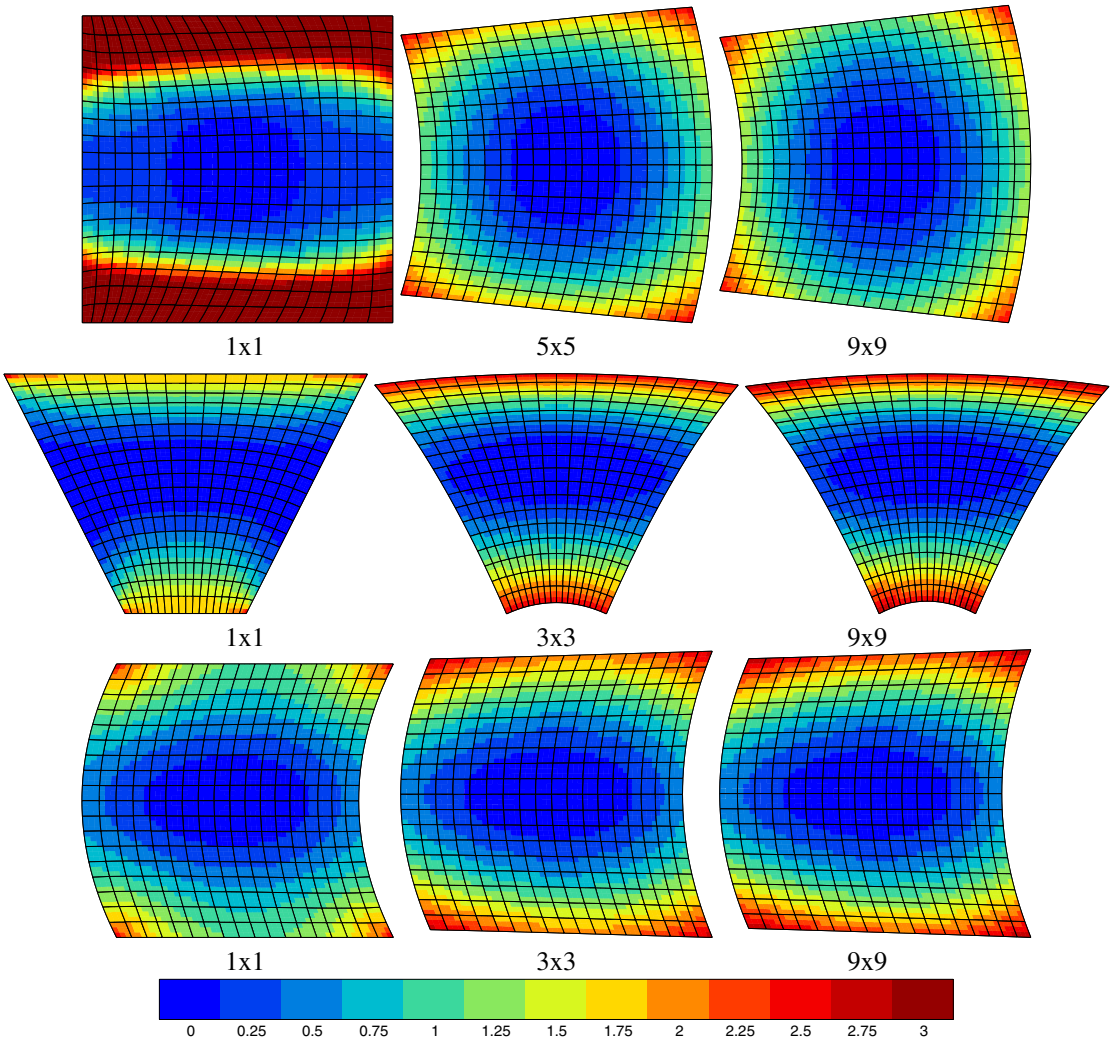

Fig. 4 (online colour at: www.zamm-journal.org) Normalised strain energy field $W(\underline{\boldsymbol{x}})/\overline{W}$ in the central unit cell when applying quadratic Dirichlet boundary conditions (15) at the remote boundary of a $N \times N$ group of cells, for $D_{111} = 1\ \text{mm}^{-1}$ (top), $D_{112} = 1\ \text{mm}^{-1}$ (middle), $D_{122} = 1\ \text{mm}^{-1}$ (bottom). The considered material is a homogeneous material. An arbitrary unit cell of size $l = 1$ mm has been chosen.

A homogeneous square unit cell of edge length 1 mm has been chosen arbitrarily. The polynomial (15) has been prescribed to this single volume and to "assemblies" of $N \times N$ such unit cells. The fields of normalised strain energy in the central unit are given in Fig. 4. They show that the property of the first order polynomial does not pertain to the quadratic polynomial, for the three investigated loading conditions. However a converged solution exists in the central cell that differs from the prescribed quadratic polynomial. In other words the fluctuation does not vanish even for this homogeneous medium.

This fact can be checked easily by looking for the conditions on the polynomial coefficients for the polynomial $u_i = \frac{1}{2} D_{ijk} x_j x_k$ to be a solution of a boundary value problem in a homogeneous elastic medium.

In contrast, the cubic polynomial (27) is an admissible solution for a homogeneous isotropic medium. The corresponding fluctuation identically vanishes for a homogeneous medium, as seen in Fig. 5. This admissibility has not been tested yet for the full third order polynomial.

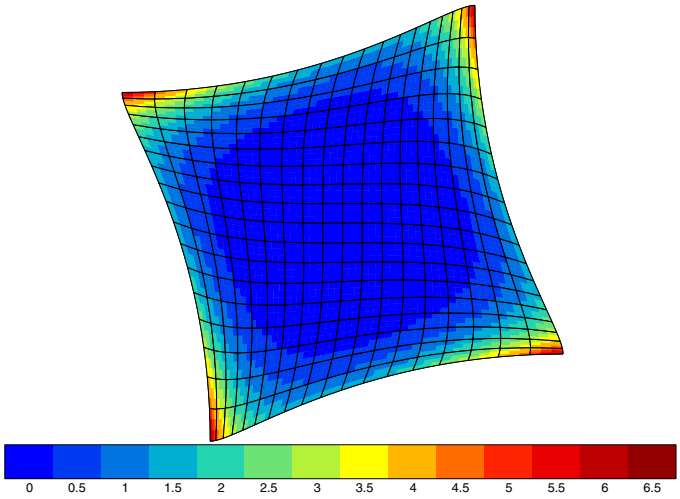

Fig. 5 (online colour at: www.zamm-journal.org) Normalised strain energy field $W(\underline{\boldsymbol{x}})/\overline{W}$ in the central unit cell when applying the cubic Dirichlet boundary conditions (27) at the remote boundary of a $N \times N$ group of cells, for $\hat{D} = 1$ mm^{-2}. The considered material is a homogeneous material. An arbitrary unit cell of size $l = 1$ mm has been chosen.

One may think of establishing some constraints on the coefficients for the polynomial to be a solution of the considered boundary value problem on the unit cell for a homogeneous medium. However, such constraints will be limited to special material symmetries of the elastic behaviour or special values of the material properties.

4.3 Convergence of the homogenization scheme for elasto-plastic media

The main advantage of the proposed extension of standard homogenization technique is that it can be used irrespective of the local material behaviour, in particular for nonlinear material behaviour. This possibility was first explored in [18] and [16] for Cosserat effective behaviour, in the case of the elastoplastic behaviour of the matrix in a composite. The response of the unit cell to the application of a mean curvature can be used to identify the material parameters of effective nonlinear constitutive equations for the macroscopic generalized continuum, or to feed an enhanced FE^2 computational strategy. However, in the latter contributions, the fluctuation was assumed to be periodic. In the present work, more general loading conditions are considered including all 2D strain gradient loading conditions, and no assumption is made regarding the fluctuation term.

For that purpose, the computational strategy for the determination of the representative volume element size adopted in the two previous sections, is applied to the same composite but assuming elastic–plastic behaviour for the matrix grid material. The constitutive equations are based on standard J_2-elastoplasticity with linear isotropic hardening. The evolution of the yield strength is $R = R_0 + Hp$, p being the cumulative plastic strain. We take: $R_0 = 100$ MPa, $H = 2000$ MPa. The $N \times N$ groups of cells are subjected to the quadratic boundary conditions (15), with, respectively, $D_{111}, D_{112}, D_{122}$ varying from 0 to 0.1 mm^{-1}, the remaining coefficients being set to zero. The maximum loading of 0.1 mm^{-1} is such that the reached plastic strain values remain compatible with the small strain framework.

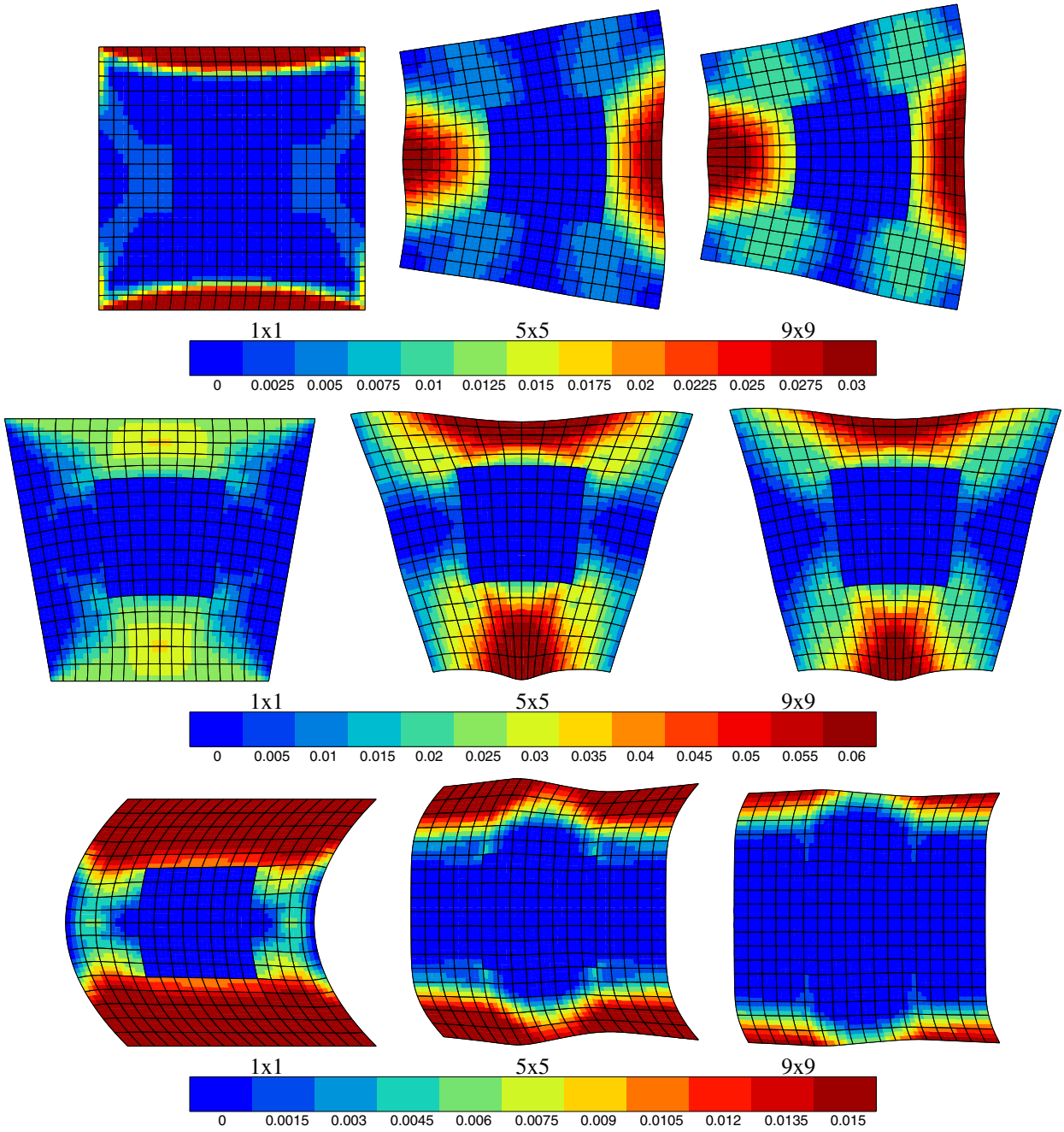

Fig. 6 (online colour at: www.zamm-journal.org) Cumulative plastic strain field in the central unit cell when applying quadratic Dirichlet boundary conditions (15) at the remote boundary of a $N \times N$ group of cells, for $D_{111} = 0.1\ \mathrm{mm}^{-1}$ (top), $D_{112} = 0.1\ \mathrm{mm}^{-1}$ (middle), $D_{122} = 0.1\ \mathrm{mm}^{-1}$ (bottom). The matrix phase is elastoplastic with linear hardening. For the illustration, the deformed state has been magnified by a factor of 10.

The Fig. 6 shows that the cumulative strain field converges if the number N of unit cells inside the volume element is increased. The final deformed states are strongly different from the linear case of Fig. 2. It can be seen that a fluctuation field develops when compared to the direct application of the quadratic conditions on the unit cell. Plasticity is found to be localized in narrow zones.

Note that such a convergence of the plastic strain state does not occur if perfect plasticity is considered because the nonlinear loading conditions induce strong plastic strain localization that are more and more intense when the size of the group of cell is increased. In particular shear bands form starting from the corners of the square volume element and intersect in the central cell. This is not presented here for the sake of brevity.

4.4 Characterisation of the fluctuation field

The proposed computational method makes it possible to fully characterize the fluctuation field from the numerical simulations. For that purpose, we compute the perturbation $\underline{\boldsymbol{v}}$ from the converged state of the central unit cell remotely subjected to the individual quadratic polynomial

$$\underline{\boldsymbol{v}}^{FE}(\underline{\boldsymbol{x}}) = \underline{\boldsymbol{u}}^{FE}(\underline{\boldsymbol{x}}) - \frac{1}{2}\underset{\sim}{\boldsymbol{D}} : \underline{\boldsymbol{x}} \otimes \underline{\boldsymbol{x}}\,, \tag{53}$$

where the exponent FE stands for the Finite Element results.

We can now compare the values that the fluctuation $\underline{\boldsymbol{v}}^{FE}$ takes at homologous points of the left and right edges, and on the bottom and top edges, of the central unit cell of Fig. 1 (left). The corresponding curves are drawn for both components v_1, v_2 for all three loading conditions $D_{111} = 1$ mm^{-1}, $D_{112} = 1$ mm^{-1} and $D_{122} = 1$ mm^{-1}, in Figs. 7, 8, and 9,

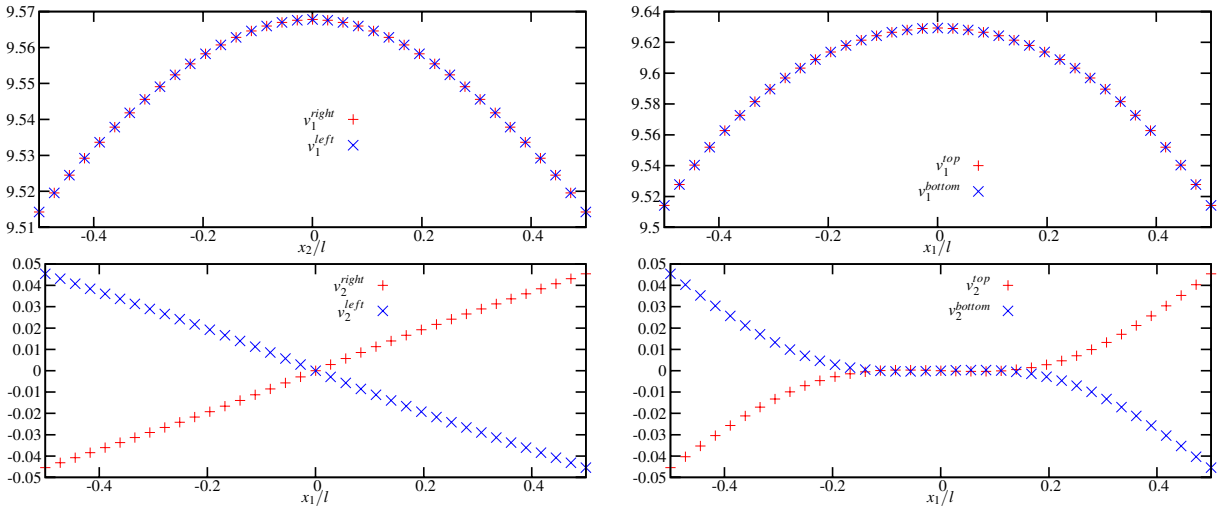

Fig. 7 (online colour at: www.zamm-journal.org) Components of the fluctuation field $\underline{\boldsymbol{v}}$ on the edges of the central unit cell for remotely prescribed quadratic boundary conditions with $D_{111} = 1$ mm^{-1}.

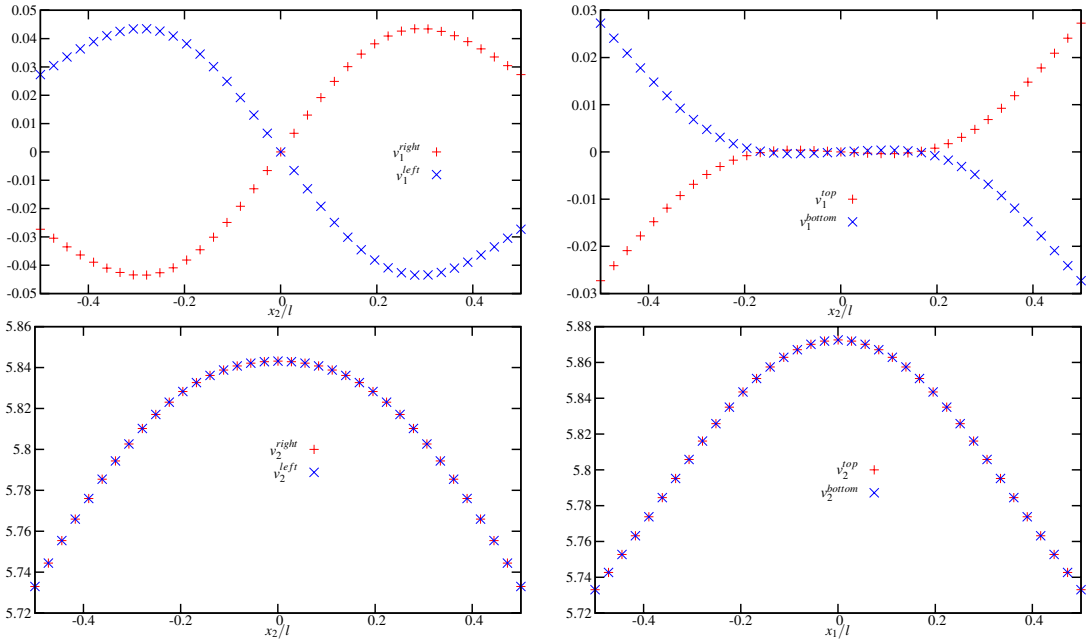

Fig. 8 (online colour at: www.zamm-journal.org) Components of the fluctuation field $\underline{\boldsymbol{v}}$ on the edges of the central unit cell for remotely prescribed quadratic boundary conditions with $D_{112} = 1$ mm^{-1}.

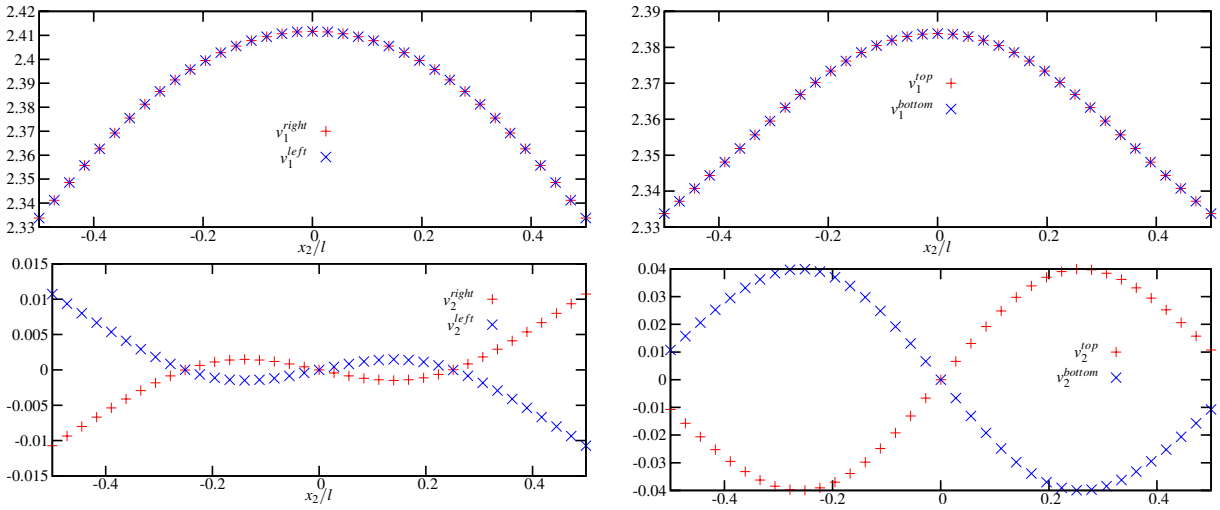

Fig. 9 (online colour at: www.zamm-journal.org) Components of the fluctuation field $\underline{\boldsymbol{v}}$ on the edges of the central unit cell for remotely prescribed quadratic boundary conditions with $D_{122} = 1\ \mathrm{mm}^{-1}$.

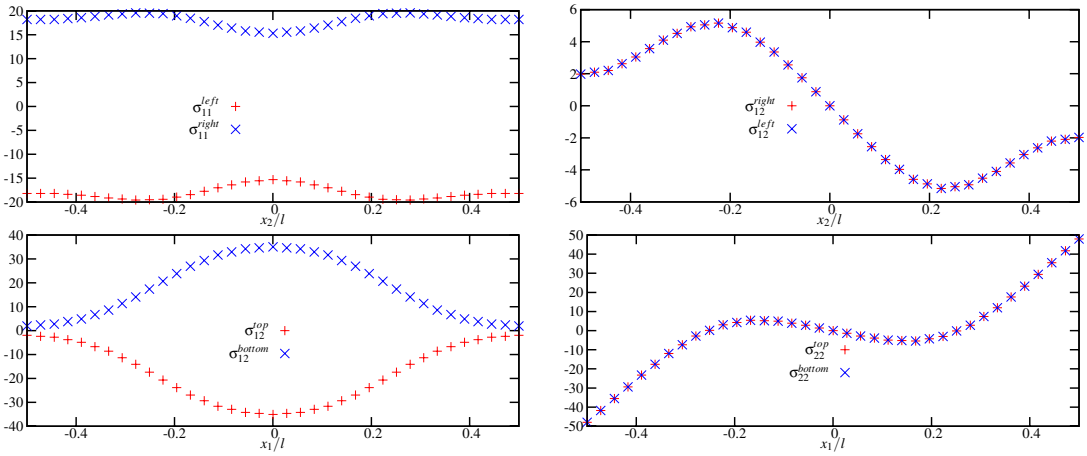

Fig. 10 (online colour at: www.zamm-journal.org) Stress components involved contributing to the traction vectors at the edges of the central unit cell for quadratic remote loading of the cell assembly with $D_{111} = 1\ \mathrm{mm}^{-1}$.

Table 2 Mean work of internal forces $\overline{W}$ over the central unit cell and the contributions of the polynomial and of the fluctuation for three overall loading conditions.

	$\overline{W}$ (MPa)	W_D (MPa)	W_v (MPa)	$\lvert W_v/\overline{W}\rvert$
$D_{111} = 1\ \mathrm{mm}^{-1}$	461.	1780.	−1319.	2.86
$D_{112} = 1\ \mathrm{mm}^{-1}$	13890.	20965.	−7075.	0.51
$D_{122} = 1\ \mathrm{mm}^{-1}$	1762.	2760.	−998.	0.57

respectively. For the loading conditions $D_{111} = 1\ \mathrm{mm}^{-1}$ and $D_{122} = 1\ \mathrm{mm}^{-1}$, we find that v_1 is periodic whereas v_2 is anti-periodic. For the loading $D_{112} = 1\ \mathrm{mm}^{-1}$, v_2 is periodic whereas v_1 is anti-periodic. As a result, the superposition of the full quadratic polynomial, i.e. including all terms, will lead to a non-periodic fluctuation.

The question of the anti-periodicity of the traction vector at the boundary of the unit cell was raised in Sect. 2.5. A definite answer can now be given from the numerical results. The traction vector on the vertical (resp. horizontal) edges of the unit cell of Fig. 1(left) involves the components σ_{11} and σ_{12} (resp. σ_{12} and σ_{22}). These components are plotted along the horizontal and vertical edges in Figs. 10, 11, and 12, for the three individual loading conditions. For the loading conditions $D_{111} = 1\ \mathrm{mm}^{-1}$ and $D_{122} = 1\ \mathrm{mm}^{-1}$, the component t_2 of the traction vector is found to be anti-periodic whereas the component t_1 is periodic. The reverse holds for the loading $D_{112} = 1\ \mathrm{mm}^{-1}$. Again, the numerical example proves that the traction is generally not anti-periodic, contrary to the case of classical homogenisation.

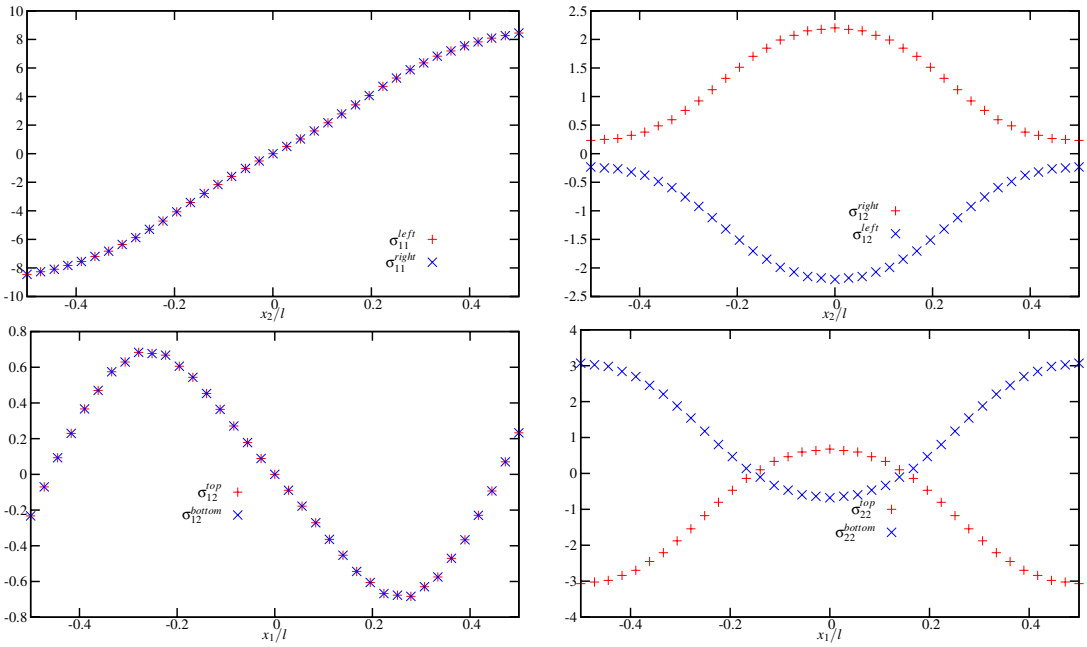

Fig. 11 (online colour at: www.zamm-journal.org) Stress components involved contributing to the traction vectors at the edges of the central unit cell for quadratic remote loading of the cell assembly with $D_{112} = 1\ \mathrm{mm}^{-1}$.

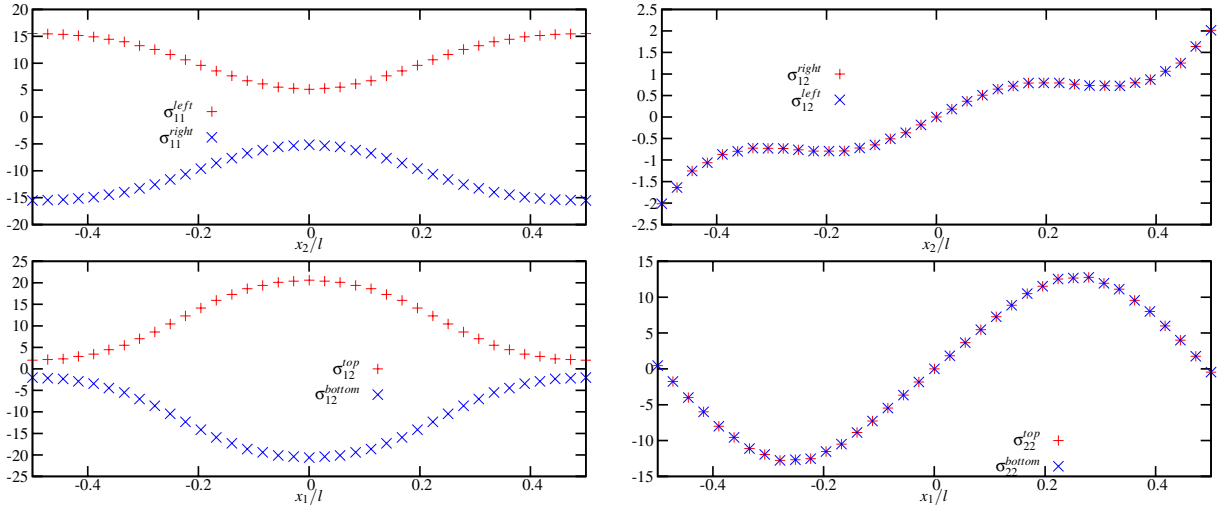

Fig. 12 (online colour at: www.zamm-journal.org) Stress components involved contributing to the traction vectors at the edges of the central unit cell for quadratic remote loading of the cell assembly with $D_{122} = 1\ \mathrm{mm}^{-1}$.

4.5 Overall contribution of the fluctuation to the energy and to the macroscopic strain gradient

The numerical example can also be used to evaluate the contribution of the fluctuation field to the overall strain energy inside the central unit cell. In classical periodic homogenisation, this contribution is known to vanish. Does this result pertain for quadratic conditions? The strain energy associated with the displacement field $\underline{\boldsymbol{u}} = \underline{\boldsymbol{u}}^* + \underline{\boldsymbol{v}}$ given by (18) is computed as

$$\begin{aligned} \overline{W} = \langle \underset{\sim}{\boldsymbol{\sigma}} : \underset{\sim}{\boldsymbol{\varepsilon}}(\underline{\boldsymbol{u}}) \rangle &= \langle \underset{\sim}{\boldsymbol{\sigma}} : \underset{\sim}{\boldsymbol{\varepsilon}}(\underline{\boldsymbol{u}}^*) \rangle + \langle \underset{\sim}{\boldsymbol{\sigma}} : \underset{\sim}{\boldsymbol{\varepsilon}}(\underline{\boldsymbol{v}}) \rangle \\ &= \langle \sigma_{ij} x_k \rangle D_{ijk} + \langle \sigma_{ij} v_{i,j} \rangle \\ &= W_D + W_v, \end{aligned} \tag{54}$$

where averaging is performed over the unit cell and were $E_{ij} = 0$ was taken for conciseness. The contribution due to $\underset{\sim}{\boldsymbol{D}}$ is W_D and the one associated with the fluctuation is W_v.

In the considered numerical example, the strain energy associated with the fluctuation is computed as a post-processing of the Finite Element simulations

$$W_v = \overline{W}^{FE} - \langle \sigma_{ij}^{FE} x_k \rangle D_{ijk}. \tag{55}$$

The different contributions are reported in Table 2. The results show that the contribution W_v does not vanish. Far from being negligible, it represents half of the total energy and even more. The contribution is negative so that the final strain energy is significantly smaller than W_D.

Similarly, we can evaluate the contribution of the fluctuation to the overall microdeformation gradient by computing

$$\underset{\approx}{\boldsymbol{K}}^T(\underline{\boldsymbol{v}}) = \underset{\approx}{\boldsymbol{K}}^T - \underset{\approx}{\boldsymbol{D}} = \langle \underline{\boldsymbol{u}}^{FE} \otimes \boldsymbol{\nabla}_x \otimes \underline{\boldsymbol{x}} \rangle \cdot \underset{\sim}{\boldsymbol{A}}^{-1} - \underset{\approx}{\boldsymbol{D}} \tag{56}$$

from the Finite Element results and from Eq. (45). It can be deduced from the values in Table 1. Again, far from being negligible, the contribution $\underset{\approx}{\boldsymbol{K}}(\underline{\boldsymbol{v}})$ is found to be a significant part of the total microdeformation gradient.

5 Conclusions

Generalized continuum approaches become efficient when the hypothesis of separation of scales between the macro and micro-levels is about to fail. If this condition fails completely, i.e. when the wave length of the variation of the macro strain and stress fields is equal or below the size of the material's heterogeneities, the only alternative is to abandon homogenization and to perform large scale computations of material domains including all relevant heterogeneities.

In the present contribution, we have proposed a critical analysis of the current endeavour for constructing a homogeneous equivalent generalised continuum replacing a composite Cauchy material. The introduction of non-homogeneous, especially polynomial, boundary conditions to the composite unit cell has been discussed as an heuristic extension of the classical homogenisation scheme. The objective was to relate the coefficients of such polynomials to the generalized strain measures of the macroscopic extended continuum. A very general continuum approach has been considered at the macro-scale, namely the micromorphic continuum, because it can account for both Cosserat rotational effects and stretching mechanisms that are important for instance in compressible materials. Explicit definitions of the macroscopic degrees of freedom and of their gradient have been put forward. It has been established that the relations between the polynomial of second to fourth order and the microdeformation and microdeformation gradient actually involve the essential contribution of a fluctuation field which has hardly been discussed in the past literature on the subject of higher order homogenization.

A computational strategy has been illustrated in the case of a simple elastic composite in order to unambiguously determine this fluctuation field. It consists in applying quadratic and cubic Dirichlet boundary conditions at the boundary of a larger and larger volume of the composite material, i.e. containing a growing number of unit cells, until a stabilised stress-strain field is reached in a central unit cell far from the outer boundary. This is the proposed definition of the representative volume element size for polynomial boundary conditions. In the case of linear elasticity, the superposition principle can be used to impose the wanted microdeformation gradient to the central unit cell. The earlier approaches proposed in the literature, that mainly rely on vanishing or periodic fluctuations, turn out to be inaccurate in the application of well-suited boundary conditions and determination of overall general stress and strain quantities. A consequence is that it is not known yet which boundary conditions could be prescribed to the perturbation at the boundary of a single unit cell in order to induce the proper displacement field without considering larger assemblies of cells. A FE^2 is therefore no longer possible.

The question of validation of the proposed approach by means of comparisons between full field and homogenized computations has not been addressed here for the sake of brevity. Such comparisons exist in the literature and are promising [12, 16, 17, 22, 32, 38]. They also show the limitations of the approach since it may fail for some special loading conditions that are typically not accounted for by the chosen polynomials. This is a situation similar to that encountered for the development of improved beam and shell models.

Many open questions remain to be solved for the proposed scheme to represent a useful and sound extension of classical homogenization procedure. In particular, only displacement based conditions have been considered yet and stress-based boundary conditions are still missing. The reason lies in the fact that it is difficult to devise non-homogeneous stress-based conditions fulfilling the requirements of balance of momentum and moment of momentum on the unit cell. Only quadratic displacement boundary conditions have been illustrated in the numerical example and the work remains to be done for determining the proper coefficients of the third and fourth order polynomials to control the overall microdeformation and microdeformation gradient.

Also, an essential question in extending homogenisation methods is the derivation of the higher order boundary conditions to be prescribed at the macro-scale for the microdeformation and associated double forces. Similar question arises for

the boundary conditions in the case of composite beams and plates, which are very often set rather intuitively. A general homogenization procedure is still missing to derive the higher order boundary conditions from the conditions at the microscale. In an heuristic manner, zero microdeformation will be applied at a clamped boundary, whereas simple and double traction free conditions will be applied to free surfaces. Derivation of more precise conditions remain a research topic.

When the fluctuation field is taken into account in the way put forward in this work, the previously proposed identification procedures for the higher order elastic constants have to be revised. For instance, the following strain energy equivalence will be considered to construct the elastic second gradient medium

$$\langle \underset{\sim}{\boldsymbol{\sigma}} : \underset{\sim}{\boldsymbol{\varepsilon}} \rangle_{V(0)} = \langle \underset{\sim}{\boldsymbol{\sigma}} \rangle : \underset{\sim}{\boldsymbol{E}} + \langle \underset{\sim}{\boldsymbol{\sigma}} \otimes \underline{\boldsymbol{x}} \rangle \vdots \underline{\underline{\boldsymbol{D}}} + \langle \underset{\sim}{\boldsymbol{\sigma}} : \underline{\boldsymbol{v}} \otimes \boldsymbol{\nabla}_x \rangle_{V(0)} = \underset{\sim}{\boldsymbol{E}} : \underset{\approx}{\boldsymbol{C}}^{eff} : \underset{\sim}{\boldsymbol{E}} + \underset{\sim}{\boldsymbol{K}} \vdots \underset{\approx}{\underset{\sim}{\boldsymbol{A}}}^{eff} \vdots \underset{\sim}{\boldsymbol{K}}, \tag{57}$$

where the effective second gradient properties are the tensors $\underset{\approx}{\boldsymbol{C}}^{eff}$ and $\underset{\approx}{\underset{\sim}{\boldsymbol{A}}}^{eff}$ of elastic moduli to be identified from several loading conditions. In general, the material will exhibit anisotropic overall properties. Elasticity symmetry classes and corresponding independent moduli have already been determined for tensors of order 6 in [3, 4].

The main advantage of the proposed polynomial approach compared to more rigorous asymptotic methods lies in the fact that the technique is readily applicable if the materials in the unit cell exhibit nonlinear behaviour. A first illustration has been given in Sect. 4.3. More generally, the approach should be used to identify the effective material parameters arising in nonlinear constitutive equations for micromorphic media. Such constitutive frameworks have been developed for elasto-viscoplasticity in the references [13, 23, 29, 30, 45, 49] and could be identified by means of the generalized homogenization method.

Acknowledgements Some aspects of this work are part of a CPR on Multifonctional Architectured Materials funded by CNRS, Arcelor-Mittal and EDF. This support is gratefully acknowledged.

References

[1] J. Altenbach, H. Altenbach, and V. A. Eremeyev, On generalized Cosserat-type theories of plates and shells: a short review and bibliography, Arch. Appl. Mech. **80**, 73–92 (2010).
[2] A. Anthoine, Second-order homogenisation of functionally graded materials, Int. J. Solids Struct. **47**, 1477–1489 (2010).
[3] N. Auffray, R. Bouchet, and Y. Bréchet, Derivation of anisotropic matrix for bi-dimensional strain-gradient elasticity behavior, Int. J. Solids Struct. **46**, 440–454 (2009).
[4] N. Auffray, R. Bouchet, and Y. Bréchet, Strain gradient elastic homogenization of bidimensional cellular media, Int. J. Solids Struct. **47**, 1698–1710 (2010).
[5] D. Besdo, Towards a Cosserat-theory describing motion of an originally rectangular structure of blocks, Arch. Appl. Mech. **80**, 25–45 (2010).
[6] J. Besson, G. Cailletaud, J. L. Chaboche, S. Forest, and M. Blétry, Non-Linear Mechanics of Materials (Series: Solid Mechanics and its Applications, Vol. 167, ISBN: 978-90-481-3355-0, (Springer, Berlin, Heidelberg, New York, 2009) p. 433.
[7] C. Boutin, Microstructural effects in elastic composites, Int. J. Solids Struct. **33**, 1023–1051 (1996).
[8] F. Bouyge, I. Jasiuk, S. Boccara, and M. Ostoja-Starzewski, A micromechanically based couple-stress model of an elastic orthotropic two-phase composite, Eur. J. Mech. A, Solids **21**, 465–481 (2002).
[9] F. Bouyge, I. Jasiuk, and M. Ostoja-Starzewski, A micromechanically based couple-stress model of an elastic two-phase composite, Int. J. Solids Struct. **38**, 1721–1735 (2001).
[10] D. Branke, J. Brummund, G. Haasemann, and V. Ulbricht, Obtaining Cosserat material parameters by homogenization of a cauchy continuum, PAMM, Proc. Appl. Math. Mech. **9**, 425–426 (2009).
[11] H. Chen, X. Liu, G. Hu, and H. Yuan, Identification of material parameters of micropolar theory for composites by homogenization method, Comput. Mater. Sci. **46**, 733–737 (2009).
[12] M. L. De Bellis and D. Addessi, A Cosserat based multi–scale model for masonry structures, Int. J. Multiscale Comput. Eng., in press (2010).
[13] T. Dillard, S. Forest, and P. Ienny, Micromorphic continuum modelling of the deformation and fracture behaviour of nickel foams, Eur. J. Mech. A, Solids **25**, 526–549 (2006).
[14] K. Enakoutsa and J. B. Leblond, Numerical implementation and assessment of the glpd micromorphic model of ductile rupture, Eur. J. Mech. A, Solids **28**, 445–460 (2009).
[15] A. C. Eringen and E. S. Suhubi, Nonlinear theory of simple microelastic solids, Int. J. Engng Sci. **2**, 189–203, 389–404 (1964).
[16] F. Feyel, A multilevel finite element method (FE2) to describe the response of highly non-linear structures using generalized continua, Comput. Methods Appl. Mech. Eng. **192**, 3233–3244 (2003).
[17] S. Forest, Mechanics of generalized continua: Construction by homogenization, J. Phys. IV **8**, Pr4-39-48 (1998).
[18] S. Forest, Aufbau und Identifikation von Stoffgleichungen für höhere Kontinua mittels Homogenisierungsmethoden, Tech. Mech. **19**(4), 297–306 (1999).
[19] S. Forest, Homogenization methods and the mechanics of generalized continua, Part 2, Theor. Appl. Mech. **28–29**, 113–143 (2002).

[20] S. Forest, The micromorphic approach for gradient elasticity, viscoplasticity and damage, ASCE J. Eng. Mech. **135**, 117–131 (2009).
[21] S. Forest, F. Pradel, and K. Sab, Asymptotic analysis of heterogeneous Cosserat media, Int. J. Solids Struct. **38**, 4585–4608 (2001).
[22] S. Forest and K. Sab, Cosserat overall modeling of heterogeneous materials, Mech. Res. Commun. **25**, 449–454 (1998).
[23] S. Forest and R. Sievert, Elastoviscoplastic constitutive frameworks for generalized continua, Acta Mech. **160**, 71–111 (2003).
[24] S. Forest and R. Sievert, Nonlinear microstrain theories, Int. J. Solids Struct. **43**, 7224–7245 (2006).
[25] M. G. D. Geers, V. G. Kouznetsova, and W. A. M. Brekelmans, Gradient-enhanced computational homogenization for the micro–macro scale transition, J. Phys. IV **11**, Pr5-145-152 (2001).
[26] P. Germain, The method of virtual power in continuum mechanics. Part 2: Microstructure, SIAM J. Appl. Math. **25**, 556–575 (1973).
[27] J. D. Goddard, Mathematical Models of Granular Matter, edited by P. Mariano, G. Capriz, and P. Giovine, Chap. From Granular Matter to Generalized Continuum, Vol. 1937 of Lecture Notes in Mathematics, 2008 (Springer, Berlin, 2008) pp. 1–20.
[28] M. Gologanu, J. B. Leblond, and J. Devaux, Continuum Micromechanics, CISM Courses and Lectures Vol. 377, Chap. Recent Extensions of Gurson's Model for Porous Ductile Metals, (Springer, Berlin, 1997) pp. 61–130.
[29] P. Grammenoudis and C. Tsakmakis, Micromorphic continuum Part I: Strain and stress tensors and their associated rates, Int. J. Non-Linear Mech. **44**, 943–956 (2009).
[30] P. Grammenoudis, C. Tsakmakis, and D. Hofer, Micromorphic continuum Part II: Finite deformation plasticity coupled withdamage, Int. J. Non-Linear Mech. **44**, 957–974 (2009).
[31] C. B. Hirschberger and P. Steinmann, Classification of concepts in thermodynamically consistent generalized plasticity, ASCE J. Eng. Mech. **135**, 156–170 (2009).
[32] R. Jänicke and S. Diebels, A numerical homogenisation strategy for micromorphic continua, Nuovo Cimento C **32**, 121–132 (2009).
[33] R. Jänicke, S. Diebels, H. G. Sehlhorst, and A. Düster, Two-scale modelling of micromorphic continua, Contin. Mech. Thermodyn. **21**, 297–315 (2009).
[34] T. Kanit, F. Nguyen, S. Forest, D. Jeulin, M. Reed, and S. Singleton, Apparent and effective physical properties of heterogeneous materials: representativity of samples of two materials from food industry, Comput. Methods in Appl. Mech. Eng. **195**, 3960–3982 (2006).
[35] V. Kouznetsova, M. G. C. Geers, and W. A. M. Brekelmans, Size of a RVE in a second order computational homozenization framework, Int. J. Multiscale Comput. Eng. **2**, 575–598 (2004).
[36] V. G. Kouznetsova, M. G. D. Geers, and W. A. M. Brekelmans, Multi-scale constitutive modelling of heterogeneous materials with a gradient-enhanced computational homogenization scheme, Int. J. Numer. Methods Eng. **54**, 1235–1260 (2002).
[37] V. G. Kouznetsova, M. G. D. Geers, and W. A. M. Brekelmans, Multi-scale second-order computational homogenization of multiphase materials : A nested finite element solution strategy, Comp. Methods Appl. Mech. Eng. **193**, 5525–5550 (2004).
[38] S. Kruch and S. Forest, Computation of coarse grain structures using a homogeneous equivalent medium, J. Phys. IV **8**, Pr8-197-205 (1998).
[39] X. Liu and G. Hu, Inclusion problem of microstretch continuum, Int. J. Eng. Sci. **42**, 849–860 (2003).
[40] C. C. Mei, J. L. Auriault, and C. O. Ng, Some applications of the homogenization theory, Adv. Appl. Mech. **32**, 277–348 (1996).
[41] R. D. Mindlin, Micro–structure in linear elasticity, Arch. Ration. Mech. Anal. **16**, 51–78 (1964).
[42] R. D. Mindlin and N. N. Eshel, On first strain gradient theories in linear elasticity, Int. J. Solids Struct. **4**, 109–124 (1968).
[43] P. Neff and S. Forest, A geometrically exact micromorphic model for elastic metallic foams accounting for affine microstructure. Modelling, existence of minimizers, identification of moduli and computational results, J. Elast. **87**, 239–276 (2007).
[44] M. Ostoja-Starzewski, S. D. Boccara, and I. Jasiuk, Couple-stress moduli and characteristic length of two-phase composite, Mech. Res. Commun. **26**, 387–396 (1999).
[45] R. A. Regueiro, On finite strain micromorphic elastoplasticity, Int. J. Solids Struct. **47**, 786–800 (2010).
[46] G. J. Rodin, Higher-order microscopic measures, J. Mech. Phys. Solids **55**, 1103–1119 (2007).
[47] G. Salerno and F. de Felice, Continuum modeling of periodic brickwork, Int. J. Solids Struct. **46**, 1251–1267 (2009).
[48] V. Sansalone, P. Trovalusci, and F. Cleri, Multiscale modeling of materials by a multifield approach: microscopic stress and strain distribution in fiber-matrix composites, Acta Mater. **54**, 3485–3492 (2006).
[49] C. Sansour, S. Skatulla, and H. Zbib, A formulation for the micromorphic continuum at finite inelastic strains, Int. J. Solids Struct. **47**, 1546–1554 (2010).
[50] P. Trovalusci and R. Masiani, Non-linear micropolar and classical continua for anisotropic discontinuous materials, Int. J. Solids Struct. **48**, 1281–1297 (2003).
[51] F. Xun, G. Hu, and Z. Huang, Size-dependence of overall in-plane plasticity for fiber composites, Int. J. Solids Struct. **41**, 4713–4730 (2004).
[52] X. Yuan, Y. Tomita, and T. Andou, A micromechanical approach of nonlocal modeling for media with periodic microstructures, Mech. Res. Commun. **35**, 126–133 (2008).
[53] L. Zybell, U. Mühlich, and M. Kuna, Constitutive equations for porous plane-strain gradient elasticity obtained by homogenization, Arch. Appl. Mech. **79**, 359–375 (2009).

